

International Journal of Modern Physics D
© World Scientific Publishing Company

HORIZON QUANTUM MECHANICS
A hitchhiker's guide to Quantum Black Holes

Roberto Casadio

*Dipartimento di Fisica e Astronomia,
Alma Mater Università di Bologna,
via Irnerio 46, 40126 Bologna, Italy
casadio@bo.infn.it*

Andrea Giugno

*Dipartimento di Fisica e Astronomia,
Alma Mater Università di Bologna,
via Irnerio 46, 40126 Bologna, Italy
andrea.giugno2@unibo.it*

Octavian Micu

*Institute of Space Science, Bucharest,
P.O. Box MG-23, RO-077125 Bucharest-Magurele, Romania
octavian.micu@space-science.ro*

Received Day Month Year

Revised Day Month Year

It is congruous with the quantum nature of the world to view the space-time geometry as an emergent structure that shows classical features only at some observational level. One can thus conceive the space-time manifold as a purely theoretical arena, where quantum states are defined, with the additional freedom of changing coordinates like any other symmetry. Observables, including positions and distances, should then be described by suitable operators acting on such quantum states. In principle, the top-down (canonical) quantisation of Einstein-Hilbert gravity falls right into this picture, but is notoriously very involved. The complication stems from allowing all the classical canonical variables that appear in the (presumably) fundamental action to become quantum observables acting on the “superspace” of all metrics, regardless of whether they play any role in the description of a specific physical system. One can instead revisit the more humble “minisuperspace” approach and choose the gravitational observables not simply by imposing some symmetry, but motivated by their proven relevance in the (classical) description of a given system. In particular, this review focuses on compact, spherically symmetric, quantum mechanical sources, in order to determine the probability they are black holes rather than regular particles. The gravitational radius is therefore lifted to the status of a quantum mechanical operator acting on the “horizon wave-function”, the latter being determined by the quantum state of the source. This formalism is then applied to several sources with a mass around the fundamental scale, which are viewed as natural

2 *R. Casadio, A. Giugno and O. Micu*

candidates of quantum black holes.

Keywords: Horizon Wave-Function; Quantum Mechanics; Black Holes.

PACS numbers:

1. Introduction

After Einstein introduced the theory of Special Relativity,¹ we have grown accustomed to thinking of the space-time as the geometrical space where things happen. In this respect, Special Relativity just adds one dimension to the three-dimensional space of Newtonian physics, which is the natural arena for describing mathematically our intuitive notion of motion, or object displacements. However, we should not forget Einstein's first great achievement came from a rethinking of the concept of time and length as being related to actual measurements, which in turn require synchronised clocks. Quantum physics emerged around the same time from the very same perspective: a proper description of atoms and elementary particles, and other phenomena mostly occurring at microscopic scales, required a more refined analysis of how variables involved in such phenomena are actually measured. Since measuring means interacting with the system under scrutiny, the uncertainty principle due to a finite Planck constant then came out as a fact of life, like the Lorentz transformations come out from the finite speed of light. This gave rise to the mathematical structure of the complex Hilbert space of states, on which observables are given by operators with suitable properties, and the outcome of any measurements could then be predicted with at best a certain probability. In Special Relativity one can nonetheless think of the space-time coordinates as being labels of actual space-time points, observables in principle, as they implicitly define an inertial observer.

Then came General Relativity,² which allows for the use of any coordinates to identify space-time points, in a way that let us describe physics again much closer to what experimentalists do. The price to pay is that space-time correspondingly becomes a manifold endowed with a general Lorentzian metric, which acts as the “potential” for the universal gravitational force. This metric, in practice, determines the causal structure that was before given by the fixed Minkowski metric, and black holes (BHs) were found in this theory. The quantisation of matter fields on these metric manifolds led to the discovery of paradoxes and other difficulties, which are often pinpointed as the smoking gun that these two theories, of Quantum matter (fields) and General Relativity, are hard to unify. But if one looks back at how these two pillars of modern physics precisely emerged from the rethinking of the interplay between a physical system and the observer, the path to follow should become clear, at least ideally: one should give up as many assumptions as possible, and set up the stage for describing the most fundamental processes that involve both. In so doing, one preliminary question we can try to address is what are the best variables to use (for each specific system), regardless of what we have come to accept as “fundamental” or “elementary”. The very concept of space-time, as a “real” entity,

should be put through this rethinking process. If the aim of our quantum theory is to describe the motion of objects, the space-time geometry is just an effective picture that we can conveniently employ in classical General Relativity, but which might be too difficult to describe fully in the quantum theory.³ In fact, the first step in this construction should be to give a clear modelling of the detection process by which we observe something somewhere: which observables should we employ then, and what are the physical restrictions we expect on them? All we wrote above is in fact nothing new. Any attempt at quantising canonically the Einstein-Hilbert action⁴⁻⁷ falls into this scheme, in which the space-time is just a mathematical arena, and the metric becomes the basic observable, along with matter variables. Unfortunately, a mathematical treatment of the so called “superspace” of wave-functions describing all the possible states of the metric is extremely complicated. In fact, DeWitt himself, in his famous 1967 paper,⁶ immediately reverted to a simplified formulation in order to apply it to cosmology. His choice was based on preserving isotropy and homogeneity of the universe at the quantum level, which leads to the Friedman-Robertson-Walker family of metrics, with one degree of freedom, the scale factor. The corresponding space of quantum states is greatly simplified and referred to as the FRW “minisuperspace”.

On the other hand, one of the most relevant scenarios where we expect a quantum theory of gravitation could lead to strong predictions is the collapse of compact objects and the possible formation of BHs. This physical process cannot be realistically modelled as isotropic or homogeneous in all of its aspects, both because of the high non-linearity of the underlying relativistic dynamics and for the presence of many mechanisms, e.g. generating outgoing radiation.⁸⁻¹¹ After the seminal papers of Oppenheimer and co-workers,^{12,13} the literature on the subject has grown immensely, but many issues are still open in General Relativity (see, e.g. Ref.,¹⁴⁻¹⁷ and references therein). This is not to mention the conceptual and technical difficulties one faces when the quantum nature of the collapsing matter is taken into account. Assuming quantum gravitational fluctuations are small, one can describe matter by means of Quantum Field Theory on the curved background space-time,¹⁸ an approach which has produced remarkable results, like the discovery of the Hawking evaporation.^{19,20} However, the use of a fixed background is directly incompatible with the description of a self-gravitating system representing a collapsing object, for which the evolution of the background and possible emergence of non-trivial causal structures cannot be reliably addressed perturbatively.

A general property of the Einstein theory is that the gravitational interaction is always attractive and we are thus not allowed to neglect its effect on the causal structure of space-time if we pack enough energy in a sufficiently small volume. This can occur, for example, if two particles (for simplicity, of negligible spatial extension and total angular momentum) collide with an impact parameter b shorter than the Schwarzschild radius corresponding to the total center-of-mass energy E

4 *R. Casadio, A. Giugno and O. Micu*

of the system, that is ^a

$$b \leq 2 \ell_{\text{p}} \frac{E}{m_{\text{p}}} \equiv r_{\text{H}} . \quad (1)$$

This hoop conjecture²¹ has been checked and verified theoretically in a variety of situations, but it was initially formulated for BHs of (at least) astrophysical sizes,^{22–24} for which the very concept of a classical background metric and related horizon structure should be reasonably safe (for a review of some problems, see the bibliography in Ref.²⁵). Whether the concepts involved in the above conjecture can also be trusted for masses approaching the Planck size, however, is definitely more challenging. In fact, for masses in that range, quantum effects may hardly be neglected (for a recent discussion, see, e.g., Ref.²⁶) and it is reasonable that the picture arising from General Relativistic BHs must be replaced in order to include the possible existence of “quantum BHs”. Although a clear definition of such objects is still missing, most would probably agree that their production cross-section should (approximately) comply with the hoop conjecture, and that they do not decay thermally (see, e.g., Refs.^{27–32}).

The main complication in studying the Planck regime is that we do not have any experimental insight thereof, which makes it very difficult to tell whether any theory we could come up with is physically relevant. We might instead start from our established concepts and knowledge of nature, and push them beyond the present experimental limits. If we set out to do so, we immediately meet with a conceptual challenge: how can we describe a system containing both Quantum Mechanical objects (such as the elementary particles of the Standard Model) and classically defined horizons? The aim of this review is precisely to show how one can introduce an operator (observable) for the gravitational radius, and define a corresponding horizon wave-function (HWF),³³ which can be associated with any localised Quantum Mechanical particle or source.^{34,35} This horizon quantum mechanics (HQM) then provides a quantitative (albeit probabilistic) condition that distinguishes a BH from a regular particle. Since this “transition” occurs around the Planck scale, the HQM represents a simple tool to investigate properties of (any models of) quantum BHs in great generality. We shall also review how the HQM naturally leads to an effective Generalised Uncertainty Principle (GUP)^{36–40} for the particle position, a decay rate for microscopic BHs,³⁶ and a variety of other results for BHs with mass around the fundamental Planck scale³² (for a review of the results obtained from the HWF for Bose-Einstein condensate models of astrophysical size BHs, see Ref.⁴¹).

The paper is organised as follows: in the next Section, we first recall a few relevant notions about horizons in General Relativity and then illustrate the main ideas that define the HQM^{33,42} and how it differs from other attempts at quantising horizon degrees of freedom; in Section 3, we apply the general HQM to the particularly

^aWe shall use units with $c = k_B = 1$, and always display the Newton constant $G = \ell_{\text{p}}/m_{\text{p}}$, where ℓ_{p} and m_{p} are the Planck length and mass, respectively, so that $\hbar = \ell_{\text{p}} m_{\text{p}}$.

simple cases of a particle described by a Gaussian wave-function at rest, electrically neutral in four³⁶ and in $(1 + D)$ dimensions (with $D = 1$ and $D > 3$),⁴³ and with electric charge in four dimensions;^{44,45} we also consider collisions of two such particles in one spatial dimension and extend the hoop conjecture into the quantum realm;⁴⁶ in Section 4, we recall a proposal for including the time evolution in the HQM⁴² and, finally, in Section 5, we comment on such findings and outline future applications.

2. Horizon Quantum Mechanics

The very first attempt at solving Einstein's field equations resulted in the discovery of the Schwarzschild metric^{47,48}

$$ds^2 = -f dt^2 + f^{-1} dr^2 + r^2 (d\theta^2 + \sin^2 \theta d\phi^2) , \quad (2)$$

with

$$f = 1 - \frac{2M}{r} , \quad (3)$$

and the appearance of the characteristic length $R_H = 2M$ associated to the source. In fact, given a spherically symmetric matter source, the Schwarzschild radius R_H measures the area of the event horizon, which makes the interior of the sphere causally disconnected from the outer portion of space-time. At the same time, Quantum Mechanics (QM) naturally associates a Compton-de Broglie wavelength to a particle. This is the minimum resolvable length scale, according to the Heisenberg uncertainty principle, and it can be roughly understood as the threshold below which quantum effects cannot be neglected. It is clear that any attempt at quantising gravity should regard those two lengths on somewhat equal grounds. We therefore start with a brief review of these concepts before discussing how to deal with them consistently in the quantum theory.

2.1. Gravitational radius and trapping surfaces

In order to introduce the relevant properties of a classical horizon, we start by writing down the most general metric for a spherically symmetric space-time as⁴⁹

$$ds^2 = g_{ij}(x^k) dx^i dx^j + r^2(x^k) (d\theta^2 + \sin^2 \theta d\phi^2) , \quad (4)$$

where r is the areal coordinate and $x^i = (x^0, x^1)$ are coordinates on surfaces where the angles θ and ϕ are constant. It is clear that all the relevant physics takes place on the radial-temporal plane and we can safely set $x^0 = t$ and $x^1 = r$ from now on. Heuristically, we can think of a (local) "apparent horizon" as the place where the escape velocity equals the speed of light, and we expect its location be connected to the energy in its interior by simple Newtonian reasoning. More technically, in General Relativity, an apparent horizon occurs where the divergence of outgoing

6 *R. Casadio, A. Giugno and O. Micu*

null congruences vanishes,⁴⁹ and the radius of this trapping surface in a spherically symmetric space-time is thus determined by

$$g^{ij} \nabla_i r \nabla_j r = 0 , \quad (5)$$

where $\nabla_i r$ is the covector perpendicular to surfaces of constant area $\mathcal{A} = 4\pi r^2$. But then General Relativity makes it very hard to come up with a sensible definition of the amount of energy inside a generic closed surface. Moreover, even if several proposals of mass functions are available,⁵⁰ there is then no simple relation between these mass functions and the location of trapping surfaces. Accidentally, spherical symmetry is powerful enough to overcome all of these difficulties, in that it allows to uniquely define the total Misner-Sharp mass as the integral of the classical matter density $\rho = \rho(x^i)$ weighted by the flat metric volume measure,

$$m(t, r) = \frac{4\pi}{3} \int_0^r \rho(t, \bar{r}) \bar{r}^2 d\bar{r} , \quad (6)$$

as if the space inside the sphere were flat. This Misner-Sharp function represents the active gravitational mass^b inside each sphere of radius r and also determines the location of trapping surfaces, since Einstein equations imply that

$$g^{ij} \nabla_i r \nabla_j r = 1 - \frac{2M}{r} , \quad (7)$$

where $M = \ell_p m/m_p$. Due to the high non-linearity of gravitational dynamics, it is still very difficult to determine how a matter distribution evolves in time and forms surfaces obeying Eq. (5), but we can claim that a classical trapping surface is found where the gravitational radius $R = 2M$ equals the areal radius r , that is

$$R_{\text{H}} \equiv 2M(t, r) = r , \quad (8)$$

which is nothing but a generalisation of the hoop conjecture (1) to continuous energy densities. Of course, if the system is static, the above radius will not change in time and the trapping surface becomes a permanent proper horizon (which is the case we shall mostly consider in the following).

It stands out that the above picture lacks of any mass threshold, since the classical theory does not yield a lower limit for the function M . Therefore, it seems that one can set the area of the trapping surface to be arbitrarily small and eventually have BHs of vanishingly small mass.

2.2. Compton length and BH mass threshold

As we mentioned above, quantum mechanics provides a length cut-off through the uncertainty in the spatial localisation of a particle. It is roughly given by the Compton length

$$\lambda_m \simeq \ell_p \frac{m_p}{m} = \frac{\ell_p^2}{M} \quad (9)$$

^bRoughly speaking, it is the sum of both matter energy and its gravitational potential energy.

if, for the sake of simplicity, we consider a spin-less point-like source of mass m . It is a well-established fact that quantum physics is a more fundamental description of the laws of nature than classical physics. This means that R_{H} only makes sense when it is not “screened” by λ_m , that is

$$R_{\text{H}} \geq \lambda_m , \quad (10)$$

and, equivalently, the BH mass must satisfy

$$m \geq m_{\text{p}} , \quad (11)$$

or $M \geq \ell_{\text{p}}$. We want to remark that the Compton length (9) can also be thought of as a quantity which rules the quantum interaction of m with the local geometry. Although it is likely that the particle's self-gravity will affect it, we still safely assume the flat space condition (11) as a reasonable order of magnitude estimate.

In light of recent developments, the common argument that quantum gravity effects should become relevant only at scales of order m_{p} or higher appears to be somewhat questionable, since the condition (11) implies that a classical description of a gravitational system with $m \gg m_{\text{p}}$ should be fairly accurate (whereas for $m \sim m_{\text{p}}$ the judge remains out). This is indeed the idea of “classicalization” in a nutshell, as it was presented in Refs.^{51,52} and, before that, of models with a minimum length and gravitationally inspired GUPs.⁵³ The latter are usually presented as fundamental principles for the reformulation of quantum mechanics in the presence of gravity, following the canonical steps that allow to bring a theory to the quantum level. In this picture, gravity would then reduce to a “kinematic effect” encoded by the modified commutators for the canonical variables. In this review, we shall instead follow a different line of reasoning: we will start from the introduction of an auxiliary wave-function that describes the horizon associated with a given localised particle, and retrieve a modified uncertainty relation as a consistent result.³⁶

2.3. Horizon Wave-Function

We are now ready to formulate the quantum mechanical description of the gravitational radius in three spatial dimensions in a general fashion.³³ For the reasons listed above, we shall only consider quantum mechanical states representing *spherically symmetric* objects, which are *localised in space*. Since we want to put aside a possible time evolution for the moment (see Section 4), we also choose states *at rest* in the given reference frame or, equivalently, we suppose that every function is only taken at a fixed instant of time. According to the standard procedure, the particle is consequently described by a wave-function $\psi_{\text{S}} \in L^2(\mathbb{R}^3)$, which we assume can be decomposed into energy eigenstates,

$$|\psi_{\text{S}}\rangle = \sum_E C(E) |\psi_E\rangle . \quad (12)$$

8 *R. Casadio, A. Giugno and O. Micu*

As usual, the sum over the variable E represents the decomposition on the spectrum of the Hamiltonian,

$$\hat{H} | \psi_E \rangle = E | \psi_E \rangle , \quad (13)$$

regardless of the specific form of the actual Hamiltonian operator \hat{H} . Note though that the relevant Hamiltonian here should be the analogue of the flat space energy that defines the Misner-Sharp mass (6). Once the energy spectrum is known, we can invert the expression of the Schwarzschild radius in Eq. (1) in order to get

$$E = m_{\text{p}} \frac{r_{\text{H}}}{2 \ell_{\text{p}}} . \quad (14)$$

We then define the (unnormalised) HWF as

$$\psi_{\text{H}}(r_{\text{H}}) = C (m_{\text{p}} r_{\text{H}}/2 \ell_{\text{p}}) , \quad (15)$$

whose normalisation is fixed by means of the Schrödinger scalar product in spherical symmetry,

$$\langle \psi_{\text{H}} | \phi_{\text{H}} \rangle = 4 \pi \int_0^{\infty} \psi_{\text{H}}^*(r_{\text{H}}) \phi_{\text{H}}(r_{\text{H}}) r_{\text{H}}^2 dr_{\text{H}} . \quad (16)$$

In this conceptual framework, we could naively say that the normalised wave-function ψ_{H} yields the probability for an observer to detect a gravitational radius of areal radius $r = r_{\text{H}}$ associated with the particle in the quantum state ψ_{S} . The sharply defined classical radius R_{H} is thus replaced by the expectation value of the operator \hat{r}_{H} . Since the related uncertainty is in general not zero, this gravitational quantity will necessarily be “fuzzy”, like the position of the source itself. In any case, we stress that the observational meaning of the HQM will appear only after we introduce a few derived quantities.

In fact, we recall that we aimed at introducing a quantitative way of telling whether the source is a BH or a regular particle. Given the wave-function ψ_{H} associated with the quantum state ψ_{S} of the source, the probability density for the source to lie inside its own horizon of radius $r = r_{\text{H}}$ will be the product of two factors, namely

$$\mathcal{P}_{<}(r < r_{\text{H}}) = P_{\text{S}}(r < r_{\text{H}}) \mathcal{P}_{\text{H}}(r_{\text{H}}) . \quad (17)$$

The first term,

$$P_{\text{S}}(r < r_{\text{H}}) = \int_0^{r_{\text{H}}} \mathcal{P}_{\text{S}}(r) dr = 4 \pi \int_0^{r_{\text{H}}} |\psi_{\text{S}}(r)|^2 r^2 dr , \quad (18)$$

is the probability that the particle resides inside the sphere of radius $r = r_{\text{H}}$, while the second term,

$$\mathcal{P}_{\text{H}}(r_{\text{H}}) = 4 \pi r_{\text{H}}^2 |\psi_{\text{H}}(r_{\text{H}})|^2 , \quad (19)$$

is the probability density that the value of the gravitational radius is r_{H} . Finally, it seems natural to consider the source is a BH if it lies inside its horizon, regardless

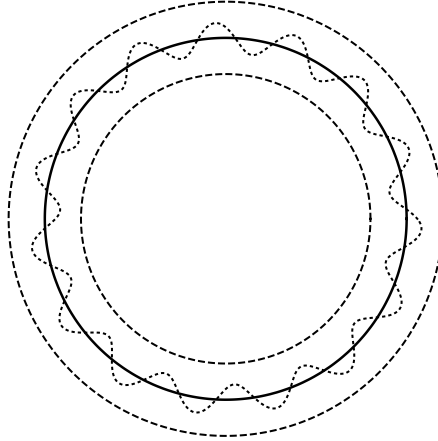


Fig. 1. Pictorial view of the HQM radial fluctuations (dashed lines) and quantum field theoretic fluctuations (dotted line) around the classical horizon radius (solid line).

of the size of the latter. The probability that the particle described by the wave-function ψ_S is a BH will then be given by the integral of (17) over all possible values of the horizon radius r_H , namely

$$P_{\text{BH}} = \int_0^\infty \mathcal{P}_<(r < r_H) dr_H, \quad (20)$$

which is the main outcome of the HQM.

In the following, we shall review the application of this construction to some simple, yet intriguing examples, in which the source is represented by Gaussian wave-functions. We anticipate that such states show very large horizon fluctuations and are not good candidates for describing astrophysical BHs³⁶ (for which extended models instead provide a better semiclassical limit⁴¹), but appear well-suited for investigating BHs around the fundamental Planck scale as unstable bound states.³²

2.4. *Alternative horizon quantizations*

It is important to remark the differences of the HQM with respect to other approaches in which the gravitational degrees of freedom of (or on) the horizon are quantised according to the background field method⁵⁴ (see, e.g. Refs.^{55–61}). In general, such attempts consider linear perturbations of the metric on this surface,⁵⁹ and apply the standard quantum field construction,¹⁸ which is what one would do with free gravitons propagating on a fixed background. Of course, the fact that the horizon is a null surface implies that these perturbative modes enjoy several peculiar properties. For instance, they can be described by a conformal field theory,⁵⁷ which one can view as the origin of the idea of BHs as holograms.^{60,61}

In the HQM, one instead only describes those spherical fluctuations of the horizon (or, more, precisely, of the gravitational radius) which are determined by the

quantum state of the source. These fluctuations therefore do not represent independent gravitational degrees of freedom, although one could suggest that they be viewed as collective perturbations in the zero point energy of the above-mentioned perturbative modes (see Fig. 1). In this respect, the HWF would be analogous to the quantum mechanical state of a hydrogen atom, whereas the perturbative degrees of freedom would be the quantum field corrections that lead to the Lamb shift.

Let us finally point out that the HQM also differs from other quantisations of the canonical degrees of freedom associated with the Schwarzschild BH metric,^{62–67} in that the quantum state for the matter source plays a crucial role in defining the HWF. The HQM is therefore complementary to most of the approaches one usually encounters in the literature. In fact, it can be combined with perturbative approaches, like it was done in Ref.,³² to show that the poles in the dressed graviton propagator³¹ can indeed be viewed as (unstable) quantum BHs.

3. Spherically symmetric Gaussian sources

We can make the previous formal construction more explicit by describing the massive particle at rest in the origin of the reference frame with the spherically symmetric Gaussian wave-function^{33,36,42}

$$\psi_S(r) = \frac{e^{-\frac{r^2}{2\ell^2}}}{(\ell\sqrt{\pi})^{3/2}}. \quad (21)$$

We shall often consider the particular case when the width ℓ (related to the uncertainty in the spatial size of the particle) is roughly given by the Compton length (9) of the particle,

$$\ell = \lambda_m \simeq \ell_p \frac{m_p}{m}. \quad (22)$$

Even though our analysis holds for independent values of ℓ and m , one expects that $\ell \geq \lambda_m$ and Eq. (22) is therefore a limiting case of maximum localisation for the source. It is also useful to recall that the corresponding wave-function in momentum space is given by

$$\tilde{\psi}_S(p) = \frac{e^{-\frac{p^2}{2\Delta^2}}}{(\Delta\sqrt{\pi})^{3/2}}, \quad (23)$$

with $p^2 = \vec{p} \cdot \vec{p}$ being the square modulus of the spatial momentum, and the width

$$\Delta = m_p \frac{\ell_p}{\ell} \simeq m. \quad (24)$$

Note that the mass m is not the total energy of the particle, and $m < \langle \hat{H} \rangle$ if the spectrum of \hat{H} is positive definite.

3.1. Neutral spherically symmetric BHs

In order to relate the momentum p to the total energy E , the latter being the analogue of the Misner-Sharp mass (6), we simply and consistently assume the relativistic mass-shell equation in flat space-time,

$$E^2 = p^2 + m^2 . \quad (25)$$

From Eq. (14), and fixing the normalisation in the inner product (16), we then obtain the HWF^{33,36,42}

$$\psi_{\text{H}}(r_{\text{H}}) = \frac{1}{4\ell_{\text{p}}^3} \sqrt{\frac{\ell^3}{\pi \Gamma\left(\frac{3}{2}, 1\right)}} \Theta(r_{\text{H}} - R_{\text{H}}) e^{-\frac{\ell^2 r_{\text{H}}^2}{8\ell_{\text{p}}^4}} , \quad (26)$$

where we defined $R_{\text{H}} = 2\ell_{\text{p}} m/m_{\text{p}}$ and the Heaviside step function appears in the above equation because $E \geq m$. Finally,

$$\Gamma(s, x) = \int_x^{\infty} t^{s-1} e^{-t} dt , \quad (27)$$

is the upper incomplete Gamma function. In general, one has two parameters, the particle mass m and the Gaussian width ℓ . The HWF will therefore depend on both and so will the probability $P_{\text{BH}} = P_{\text{BH}}(\ell, m)$, which can be computed only numerically⁴² (see also section 4).

As we mentioned previously, it seems sensible to assume $\ell \gtrsim \lambda_m$. In particular, the condition $\ell \sim m^{-1}$ in Eq. (22) precisely leads to a BH mass threshold of the form given in Eq. (11). We indeed expect that the particle will be inside its own horizon if $\langle \hat{r}^2 \rangle \lesssim \langle \hat{r}_{\text{H}}^2 \rangle$, and Eq. (11) then follows straightforwardly from $\langle \hat{r}^2 \rangle \simeq \ell^2$ and $\langle \hat{r}_{\text{H}}^2 \rangle \simeq \ell_{\text{p}}^4/\ell^2$. For example, this conclusion is illustrated in Fig. 2, where the density \mathcal{P}_{H} is plotted along with the probability density $\mathcal{P}_{\text{S}} = 4\pi r^2 |\psi_{\text{S}}(r)|^2$ for $m < m_{\text{p}}$ and $m > m_{\text{p}}$. In the former case, the horizon is more likely found within a smaller radius than the particle's, with the opposite situation occurring in the latter. As a matter of fact, the probability density (17) can be explicitly computed,

$$\mathcal{P}_{<} = \frac{\ell^3}{2\sqrt{\pi}\ell_{\text{p}}^6} \frac{\gamma\left(\frac{3}{2}, \frac{r_{\text{H}}^2}{\ell^2}\right)}{\Gamma\left(\frac{3}{2}, 1\right)} \Theta(r_{\text{H}} - R_{\text{H}}) e^{-\frac{\ell^2 r_{\text{H}}^2}{4\ell_{\text{p}}^4}} r_{\text{H}}^2 , \quad (28)$$

where $\gamma(s, x) = \Gamma(s) - \Gamma(s, x)$ is the lower incomplete Gamma function. One can integrate the density (28) for r_{H} from R_{H} to infinity and the probability (20) for the particle to be a BH is finally given by

$$P_{\text{BH}}(\ell) = \text{erf}\left(\frac{2\ell_{\text{p}}^2}{\ell^2}\right) + \frac{\sqrt{\pi}}{2} \frac{\text{erfc}\left(\frac{2\ell_{\text{p}}^2}{\ell^2}\right)}{\Gamma\left(\frac{3}{2}, 1\right)} - \frac{2\ell_{\text{p}}^2/\ell^2}{\sqrt{\pi}\Gamma\left(\frac{3}{2}, 1\right)} \frac{\left(3 + \frac{4\ell_{\text{p}}^4}{\ell^4}\right)}{\left(1 + \frac{4\ell_{\text{p}}^4}{\ell^4}\right)^2} e^{-\left(1 + \frac{4\ell_{\text{p}}^4}{\ell^4}\right)} - \frac{2\sqrt{\pi}}{\Gamma\left(\frac{3}{2}, 1\right)} T\left(\frac{2\sqrt{2}\ell_{\text{p}}^2}{\ell^2}, \frac{\ell^2}{2\ell_{\text{p}}^2}\right) , \quad (29)$$

12 *R. Casadio, A. Giugno and O. Micu*

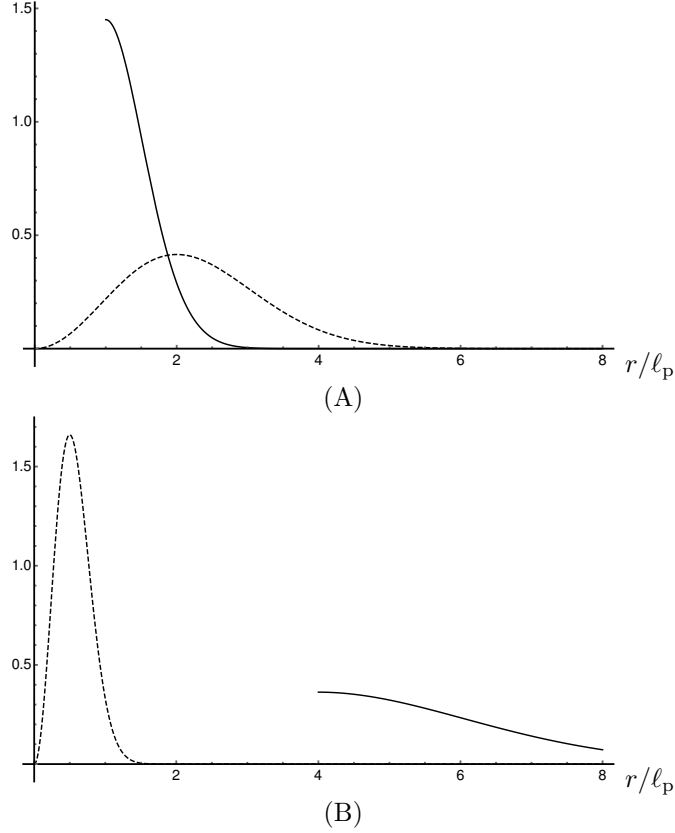


Fig. 2. Probability densities \mathcal{P}_H in Eq. (19) (solid line) and \mathcal{P}_S (dashed line) for $m = m_p/2$ (upper panel) and $m = 2m_p$ (lower panel), assuming $m \sim \ell^{-1}$.

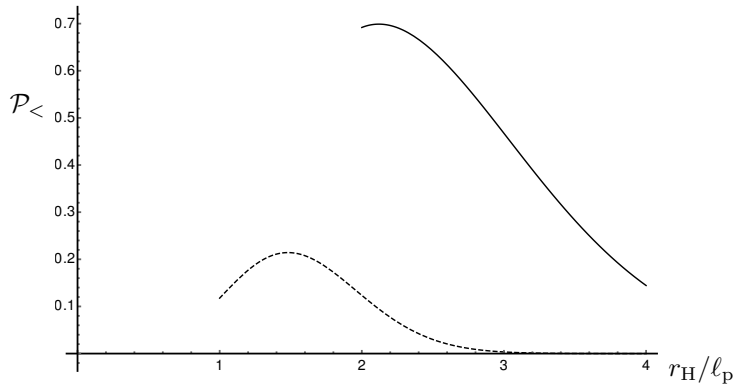


Fig. 3. Probability density $\mathcal{P}_<$ in Eq. (28) that particle is inside its horizon of radius $r_H \geq R_H = 2\ell_p m/m_p$, for $\ell = \ell_p$ (solid line) and for $\ell = 2\ell_p$ (dashed line), assuming $m \sim \ell^{-1}$.

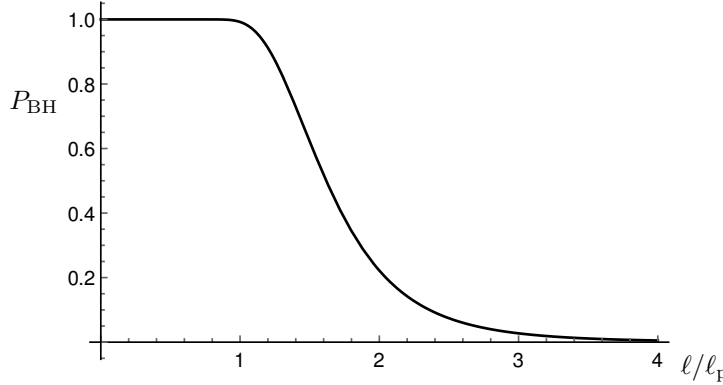


Fig. 4. Probability P_{BH} in Eq. (29) that particle of width $\ell \sim m^{-1}$ is a BH.

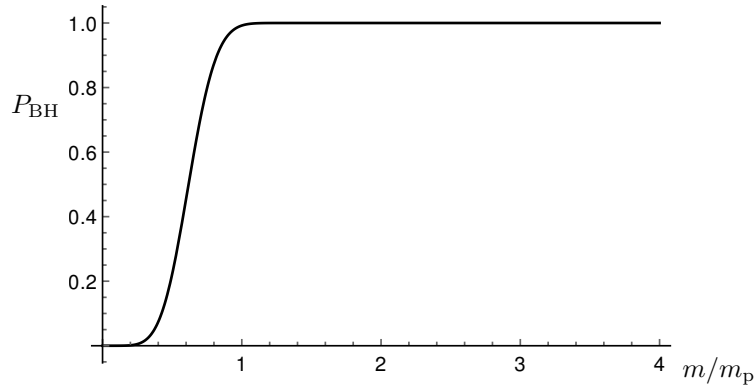


Fig. 5. Probability P_{BH} in Eq. (29) that particle of mass $m \sim \ell^{-1}$ is a BH.

where T is the Owen's function (A.7)^c. Since we are assuming that $\ell/\ell_{\text{p}} = m_{\text{p}}/m$, this probability can also be written as a function of the mass m as

$$\begin{aligned}
 P_{\text{BH}}(m) = & \operatorname{erf}\left(\frac{2m^2}{m_{\text{p}}^2}\right) + \frac{\sqrt{\pi}}{2} \frac{\operatorname{erfc}\left(\frac{2m^2}{m_{\text{p}}^2}\right)}{\Gamma\left(\frac{3}{2}, 1\right)} - \frac{2m^2/m_{\text{p}}^2}{\sqrt{\pi}\Gamma\left(\frac{3}{2}, 1\right)} \frac{\left(3 + \frac{4m^4}{m_{\text{p}}^4}\right)}{\left(1 + \frac{4m^4}{m_{\text{p}}^4}\right)^2} e^{-\left(1 + \frac{4m^4}{m_{\text{p}}^4}\right)} \\
 & - \frac{2\sqrt{\pi}}{\Gamma\left(\frac{3}{2}, 1\right)} T\left(\frac{2\sqrt{2}m^2}{m_{\text{p}}^2}, \frac{m_{\text{p}}^2}{2m^2}\right). \quad (30)
 \end{aligned}$$

In Fig. 3, we plot the probability density (28), for different values of the Gaussian width $\ell \sim m^{-1}$. It is already clear that such a probability decreases with m (eventually vanishing below the Planck mass). In fact, in Fig. 4, we show the probability (29) that the particle is a BH as a function of the width $\ell \sim m^{-1}$, and

^cMore detailed calculations of cumbersome integrals are given in Appendix A. In this particular case, the variable $x = \ell r_{\text{H}}/2\ell_{\text{p}}^2$, and we made use of Eq. (A.8) with $A = 2\ell_{\text{p}}^2/\ell^2$.

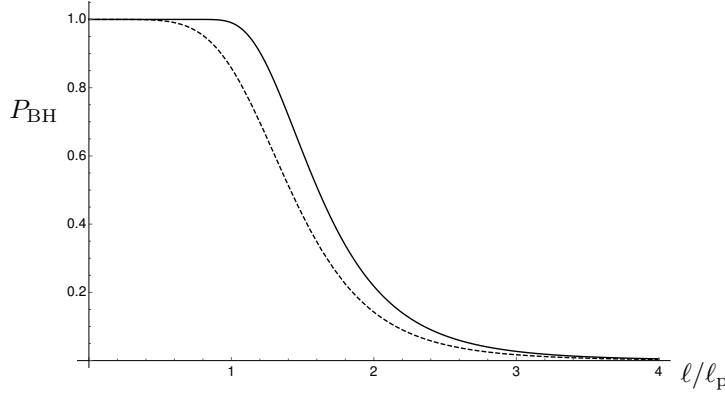


Fig. 6. Plot of exact P_{BH} in Eq. (29) (straight line) and its approximation in Eq. (32) (dashed line).

in Fig. 5 the same probability as a function of the particle mass $m \sim \ell^{-1}$. From these plots of P_{BH} , we can immediately infer that the particle is most likely a BH, namely $P_{\text{BH}} \simeq 1$, for $\ell \lesssim \ell_{\text{p}}$ or - equivalently - $m \gtrsim m_{\text{p}}$. We have therefore derived the condition (11) from a totally Quantum Mechanical picture.

We conclude by recalling that a simple analytic approximation is obtained by taking the limit $R_{\text{H}} \rightarrow 0$ in Eq. (26), namely^{33,36,42}

$$\psi_{\text{H}}(r_{\text{H}}) = \left(\frac{\ell}{2\sqrt{\pi}\ell_{\text{p}}^2} \right)^{3/2} e^{-\frac{\ell^2 r_{\text{H}}^2}{8\ell_{\text{p}}^4}}, \quad (31)$$

from which follows the approximate probability

$$P_{\text{BH}}(\ell) = \frac{2}{\pi} \left[\arctan \left(2 \frac{\ell_{\text{p}}^2}{\ell^2} \right) - \frac{2\ell^2 (\ell^4/\ell_{\text{p}}^4 - 4)}{\ell_{\text{p}}^2 (4 + \ell^4/\ell_{\text{p}}^4)^2} \right]. \quad (32)$$

Fig. 6 shows graphically that this approximation slightly underestimates the exact probability in Eq. (29).

3.1.1. *Effective GUP and horizon fluctuations*

From the Gaussian wave-function (21), we easily find that the uncertainty in the particle's size is given by

$$\begin{aligned} \Delta r^2 &\equiv 4\pi \int_0^\infty |\psi_{\text{S}}(r)|^2 r^4 dr - \left(4\pi \int_0^\infty |\psi_{\text{S}}(r)|^2 r^3 dr \right)^2 \\ &= \Delta_{\text{QM}} \ell^2, \end{aligned} \quad (33)$$

where

$$\Delta_{\text{QM}} = \frac{3\pi - 8}{2\pi}. \quad (34)$$

Analogously, the uncertainty in the horizon radius results in

$$\begin{aligned}\Delta r_{\text{H}}^2 &\equiv 4\pi \int_0^\infty |\psi_{\text{H}}(r_{\text{H}})|^2 r_{\text{H}}^4 dr_{\text{H}} - \left(4\pi \int_0^\infty |\psi_{\text{H}}(r_{\text{H}})|^2 r_{\text{H}}^3 dr_{\text{H}}\right)^2 \\ &= 4\ell_{\text{P}}^4 \left[\frac{E_{-\frac{3}{2}}(1)}{E_{-\frac{1}{2}}(1)} - \left(\frac{E_{-1}(1)}{E_{-\frac{1}{2}}(1)}\right)^2 \right] \frac{1}{\ell^2},\end{aligned}\quad (35)$$

where

$$E_n(x) = \int_1^\infty \frac{e^{-xt}}{t^n} dt, \quad (36)$$

is the generalised exponential integral. Since

$$\begin{aligned}\Delta p^2 &\equiv 4\pi \int_0^\infty |\psi_{\text{S}}(p)|^2 p^4 dp - \left(4\pi \int_0^\infty |\psi_{\text{S}}(p)|^2 p^3 dp\right)^2 \\ &= \Delta_{\text{QM}} \frac{\ell_{\text{P}}^2}{\ell^2} m_{\text{P}}^2,\end{aligned}\quad (37)$$

we can write the width of the Gaussian as $\ell^2 = \Delta_{\text{QM}} \ell_{\text{P}}^2 m_{\text{P}}^2 / \Delta p^2$, and, finally, assume the total radial uncertainty is a linear combination of Eqs. (33) and (35), thus obtaining³⁶

$$\begin{aligned}\frac{\Delta R}{\ell_{\text{P}}} &\equiv \frac{\Delta r + \xi \Delta r_{\text{H}}}{\ell_{\text{P}}} \\ &= \Delta_{\text{QM}} \frac{m_{\text{P}}}{\Delta p} + \xi \Delta_{\text{H}} \frac{\Delta p}{m_{\text{P}}},\end{aligned}\quad (38)$$

where ξ is an arbitrary coefficient (presumably of order one), and

$$\Delta_{\text{H}}^2 = \frac{4}{\Delta_{\text{QM}}} \left[\frac{E_{-\frac{3}{2}}(1)}{E_{-\frac{1}{2}}(1)} - \left(\frac{E_{-1}(1)}{E_{-\frac{1}{2}}(1)}\right)^2 \right]. \quad (39)$$

This GUP is plotted in Fig. 7 (for $\xi = 1$), and is precisely of the kind considered in Ref.,³⁷ leading to a minimum measurable length

$$\Delta R = 2\sqrt{\xi \Delta_{\text{H}} \Delta_{\text{QM}}} \ell_{\text{P}} \simeq 1.15 \sqrt{\xi} \ell_{\text{P}}, \quad (40)$$

obtained for

$$\Delta p = \sqrt{\frac{\Delta_{\text{QM}}}{\xi \Delta_{\text{H}}}} m_{\text{P}} \simeq 0.39 \frac{m_{\text{P}}}{\sqrt{\xi}}. \quad (41)$$

Of course, this is not the only possible way to define a combined uncertainty, but nothing forces us to consider a GUP instead of making direct use of the HWF.

One of the main conclusions for the HQM of Gaussian states can now be drawn from Eq. (35), that is

$$\Delta r_{\text{H}} \sim \ell^{-1} \sim m, \quad (42)$$

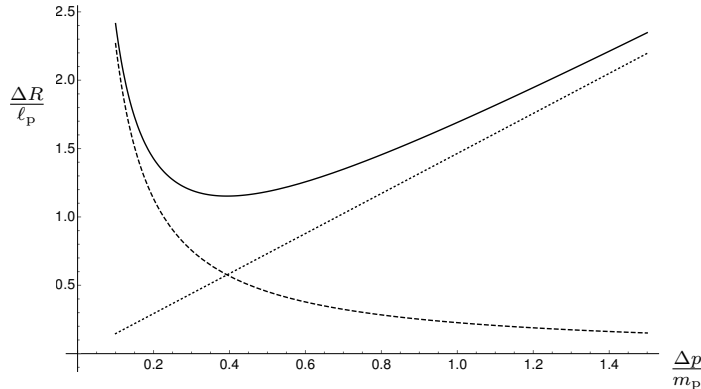


Fig. 7. Uncertainty relation (38) (solid line) as a combination of the Quantum Mechanical uncertainty (dashed line) and the uncertainty in horizon radius (dotted line).

which means the size of the corresponding horizon shows fluctuations of magnitude $\Delta r_H \sim r_H \sim R_H$. This is clearly not acceptable for BHs with mass $m \gg m_p$, which we expect to behave (semi)classically. In other words, the classical picture of a BH as the vacuum geometry generated by a (infinitely) thin matter source does not seem to survive in the quantum description, and one is led to consider alternative models for astrophysical size BHs.^{41, 68–76}

3.1.2. Quantum BH evaporation

One of the milestones of contemporary theoretical physics is the discovery that BHs radiate thermally at a characteristic temperature^{19, 20}

$$T_H = \frac{m_p^2}{8\pi m} . \quad (43)$$

However, if we try to extrapolate this temperature to vanishingly small mass M , we see that T_H diverges.

One can derive improved BH temperatures for $m \simeq m_p$ from the GUP (see Refs.^{36, 77–84} for detailed computations). Here, we just recall that one obtains^d

$$m = \frac{m_p^2}{8\pi T} + 2\pi\xi T , \quad (44)$$

with the condition $\xi > 0$, which is necessary for the existence of a minimum BH mass (see Fig. 8). We remark that this is consistent with our previous analysis, since we stated repeatedly that a particle with a mass significantly smaller than m_p should not be a BH, i.e. $P_{\text{BH}} \ll 1$ whenever $m \ll m_p$. It is straightforward to extremise (44) and get

$$m_{\min} = \sqrt{\xi} m_p , \quad T_{\max} = \frac{m_p}{4\pi\sqrt{\xi}} . \quad (45)$$

^dThe parameter ξ here is analogue, but not necessarily equal, to the parameter ξ in Eq. (38).

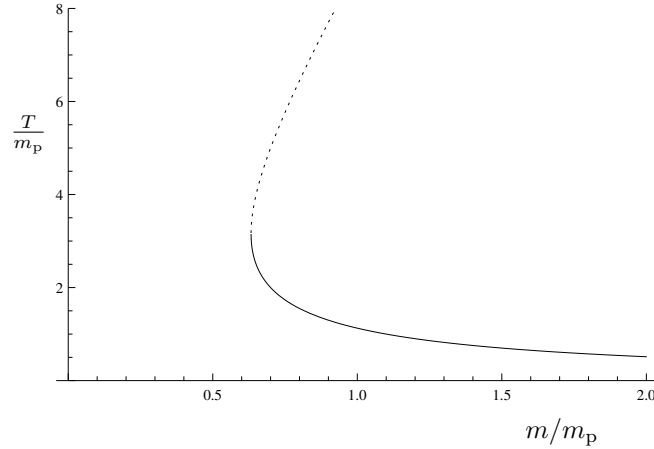


Fig. 8. Temperature vs. mass according to Eq. (44) with $\beta = 1/10$: solid line reproduces the Hawking behaviour for large $m \gg m_p$; dotted line is the unphysical branch, and their meeting point represents the BH with minimum mass.

Moreover, we can invert (44) in order to obtain $T = T(m)$ and consider the “physical” branch, which reproduces the Hawking behaviour $T = 0$ for $m \gg m_p$. When $0 < \xi < 1$ we can expand the result for m around m_p , hence

$$\begin{aligned} \frac{T}{m_p} &= \frac{1}{4\pi\xi m_p} \left(m - \sqrt{m^2 - \xi m_p^2} \right) \\ &= \frac{1 - \sqrt{1 - \xi}}{4\pi\xi} \left(1 - \frac{m - m_p}{\sqrt{1 - \xi} m_p} \right) + \mathcal{O}[(1 - m/m_p)^2] . \end{aligned} \quad (46)$$

We note that such an expansion for T is well-defined even for $\xi < 0$, suggesting that the microscopic structure of the space-time may be arranged as a lattice.⁸⁵ In the same approximation, we can also expand the canonical decay rate

$$-\frac{dm}{dt} = \frac{8\pi^3 m^2 T^4}{15 m_p^5 \ell_p} \quad (47)$$

$$\simeq \beta \frac{m^2}{m_p \ell_p} + \mathcal{O}(m - m_p) , \quad (48)$$

where $4 \cdot 10^{-5} < \beta < 7 \cdot 10^{-4}$ when $0 < \xi < 1$.³⁶

The reader may deem unlikely that an object with a mass of the order of m_p can be faithfully described by the same standard thermodynamics which arises from a (semi-)classical description of BHs. On the other hand, the HQM is specifically designed to hold in a quantum regime. We can therefore guess that the decay of a Planck size BH will be related to the probability P_T that the particle is found outside its own horizon^{e,36} Of course, if the mass $m \ll m_p$, the HWF tells us the

^eThe subscript T stands for tunnelling, which alludes to the understanding of the Hawking emission as a tunnelling process through the horizon.⁸⁶

18 *R. Casadio, A. Giugno and O. Micu*

particle is most likely not a BH to begin with, so the above interpretation must be restricted to $m \simeq m_p$ (see again Fig. 5). We first define the complementary probability density

$$\mathcal{P}_>(r > r_H) = P_S(r > r_H) \mathcal{P}_H(r_H) , \quad (49)$$

where now

$$P_S(r > r_H) = 4\pi \int_{r_H}^{\infty} |\psi_S(r)|^2 r^2 dr = \frac{2}{\sqrt{\pi}} \Gamma\left(\frac{3}{2}, \frac{r_H^2}{\ell^2}\right) . \quad (50)$$

Upon integrating the above probability density over all values of r_H , we then obtain

$$P_T(m) \simeq a - b \frac{m - m_p}{m_p} , \quad (51)$$

where $a \simeq 0.008$ and $b \simeq 0.14$ are positive constants. We can accordingly estimate the amount of particle's energy outside the horizon as

$$\Delta m \simeq m P_T \simeq a m + \mathcal{O}(m - m_p) . \quad (52)$$

On the other hand, from the time-energy uncertainty relation, $\Delta E \Delta t \simeq m_p \ell_p$, one gets the typical emission time

$$\Delta t \simeq \frac{\ell_p^2}{\Delta r_H} \simeq \ell , \quad (53)$$

employing (1) and (35). Putting the two pieces together, we find that the flux emitted by a Planck size black hole would satisfy³⁶

$$-\frac{\Delta m}{\Delta t} \simeq a \frac{m}{\ell} \simeq a \frac{m^2}{m_p \ell_p} , \quad (54)$$

whose functional behaviour agrees with the result (48) obtained from a GUP.

There is a large discrepancy between the numerical coefficients in Eq. (48) and those in Eq. (54). First, we note that Eq. (47) holds in the canonical ensemble of statistical mechanics, and the disparity may therefore arise because a Planck mass particle cannot be consistently described by standard thermodynamics, which in turn requires the BH is in quasi-equilibrium with its own radiation.^{86,87} In fact, the canonical picture does not even enforce energy conservation, which is instead granted in the microcanonical formalism.^{88,89} However, the HQM is insensitive to thermodynamics and it is therefore remarkable that the HQM and the GUP yield qualitatively similar results. In any case, the above analysis of BH evaporation is very preliminary and significant changes are to be expected when considering a better description of the microscopic structure of quantum BHs.^{32,70,73-75}

3.2. *Electrically charged sources*

An extension of the original HQM regards the case of electrically charged massive sources,⁹⁰⁻⁹⁴ and was obtained in Refs.^{44,45} from the Reissner-Nordström (RN)

metric.^{95,96} The latter is of the form (2) with

$$f = 1 - \frac{2\ell_{\text{p}} m}{m_{\text{p}} r} + \frac{Q^2}{r^2}, \quad (55)$$

where m is again the ADM mass and Q is the charge of the source. In the following, it will be convenient to employ the specific charge

$$\alpha = \frac{|Q| m_{\text{p}}}{\ell_{\text{p}} m}. \quad (56)$$

The case $\alpha = 0$ reduces to the neutral Schwarzschild metric. For $0 < \alpha < 1$, the above function f has two zeroes, namely

$$\begin{aligned} R_{\pm} &= \ell_{\text{p}} \frac{m}{m_{\text{p}}} \pm \sqrt{\left(\ell_{\text{p}} \frac{m}{m_{\text{p}}}\right)^2 - Q^2} \\ &= \ell_{\text{p}} \frac{m}{m_{\text{p}}} \left(1 \pm \sqrt{1 - \alpha^2}\right), \end{aligned} \quad (57)$$

and the RN metric therefore describes a BH. Moreover, the two horizons coincide for $\alpha = 1$ and the BH is said to be *extremal*, while the singularity is naked, i.e. accessible to an external observer, for $\alpha > 1$.

3.2.1. Inner Horizon

The case $0 < \alpha \leq 1$ was considered in Ref.,⁴⁴ where the HQM was extended for the presence of more than one trapping surface. A procedure similar to the neutral case was followed for each of the two horizon radii (57): one initially determines the HWFs and then uses them to compute the probability for each horizon to exist. Eqs. (57) is lifted to the quantum level by introducing the operators \hat{r}_{\pm} and \hat{H} , which replace their classical counterparts R_{\pm} and m . Moreover, these operators are chosen to act multiplicatively on the respective wave-functions, whereas the specific charge α remains a simple parameter (c-number)^f.

First we note the total energy \hat{H} can be expressed in terms of the horizon radii as

$$\ell_{\text{p}} \frac{\hat{H}}{m_{\text{p}}} = \frac{\hat{r}_{+} + \hat{r}_{-}}{2}, \quad (58)$$

and one also has

$$\hat{r}_{\pm} = \hat{r}_{\mp} \frac{1 \pm \sqrt{1 - \alpha^2}}{1 \mp \sqrt{1 - \alpha^2}}. \quad (59)$$

We then obtain the HWFs for r_{+} and r_{-} by expressing p from the mass-shell relation (25) in terms of the eigenvalue E of \hat{H} in Eq. (58), and then replacing one of the relations (59) into the wave-function representing the source in momentum

^fAs usual, going from the classical to the quantum realm is affected by ambiguities, and this choice is not unique.

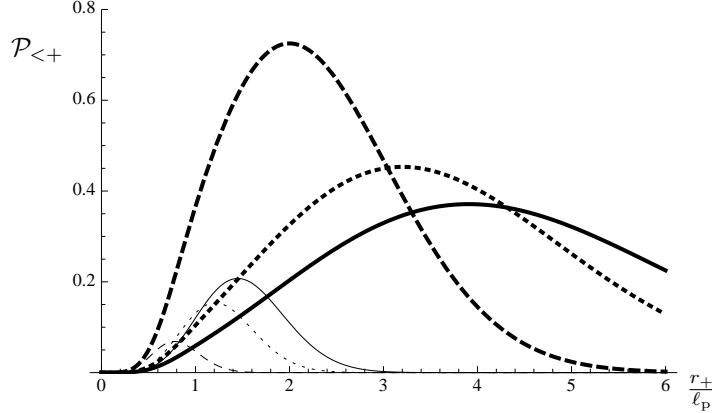


Fig. 9. Probability density $\mathcal{P}_{<+}$ in Eq. (62) that the particle is inside its outer horizon $r = r_+$, for $\ell = \ell_p/2$ (thick lines) and $\ell = 2\ell_p$ (thin lines) with $\alpha = 0.3$ (continuous lines), $\alpha = 0.8$ (dotted lines) and $\alpha = 1$ (dashed lines). For $\alpha = 1$, the two horizons coincide and $\mathcal{P}_{<-} = \mathcal{P}_{<+}$.

space, as in Eq. (23). For the usual limiting case (22), $\ell \sim m^{-1}$, it is straightforward to obtain

$$\begin{aligned} \psi_{\text{H}}(r_{\pm}) &= \sqrt{\frac{1}{2\pi\Gamma(\frac{3}{2}, 1)} \left[\frac{\ell}{\ell_p^2(1 \pm \sqrt{1 - \alpha^2})} \right]^3} \Theta(r_{\pm} - R_{\pm}) \\ &\times \exp \left\{ -\frac{\ell^2 r_{\pm}^2}{2\ell_p^4(1 \pm \sqrt{1 - \alpha^2})^2} \right\}, \end{aligned} \quad (60)$$

where the minimum radii are given by

$$R_{\pm} = \ell_p \frac{m}{m_p} \left(1 \pm \sqrt{1 - \alpha^2} \right) = \frac{\ell_p^2}{\ell} \left(1 \pm \sqrt{1 - \alpha^2} \right). \quad (61)$$

The probability densities for the source to be found inside each of the two horizons turn out to be

$$\begin{aligned} \mathcal{P}_{<\pm} &= \frac{4}{\sqrt{\pi}\Gamma(\frac{3}{2}, 1)} \left[\frac{\ell}{\ell_p^2(1 \pm \sqrt{1 - \alpha^2})} \right]^3 \Theta(r_{\pm} - R_{\pm}) \\ &\times \gamma \left(\frac{3}{2}, \frac{r_{\pm}^2}{\ell^2} \right) \exp \left\{ -\frac{\ell^2 r_{\pm}^2}{\ell_p^4(1 \pm \sqrt{1 - \alpha^2})^2} \right\} r_{\pm}^2. \end{aligned} \quad (62)$$

In the neutral case $\alpha = 0$, $\mathcal{P}_{<-}$ is of course ill-defined, while $\mathcal{P}_{<+}$ equals the probability density (28), which means that r_+ becomes the Schwarzschild radius r_{H} .

Fig. 9 shows the probability density $\mathcal{P}_{<+}$ for the massive source to reside inside the external horizon $r = r_+$ for two values of the width ℓ (above and below the Planck scale) and three values of the specific charge α . The maximum of this function clearly decreases when ℓ increases above ℓ_p or, equivalently, when m gets smaller than the Planck mass. Fig. 10 shows the analogous probability densities $\mathcal{P}_{<-}$ for

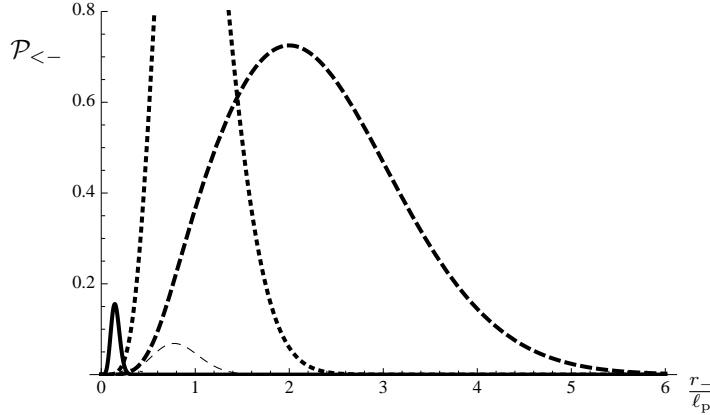


Fig. 10. Probability density $\mathcal{P}_{<-}$ in Eq. (62) that particle is inside its inner horizon $r = r_-$, for $\ell = \ell_p/2$ (thick lines) and $\ell = 2\ell_p$ (thin lines) with $\alpha = 0.3$ (continuous lines), $\alpha = 0.8$ (dotted lines) and $\alpha = 1$ (dashed lines). For $\alpha = 1$, the two horizons coincide and $\mathcal{P}_{<-} = \mathcal{P}_{<+}$.

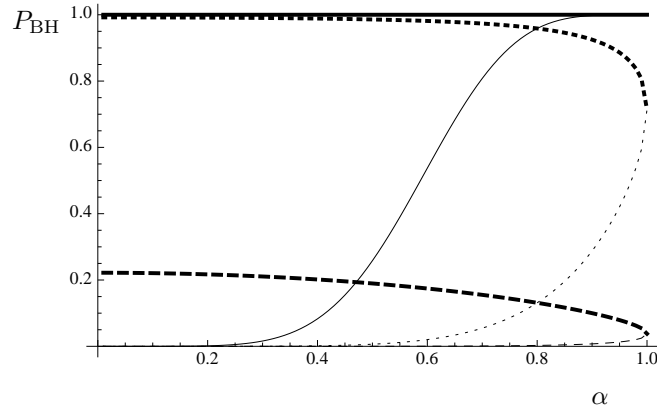


Fig. 11. Probability $P_{\text{BH}+}$ in Eq. (63) for the particle to be a BH (thick lines) and $P_{\text{BH}-}$ in Eq. (63) for the particle to be inside its inner horizon (thin lines) as functions of α for $\ell = \ell_p/2$ (continuous line), $\ell = \ell_p$ (dotted line) and $\ell = 2\ell_p$ (dashed line). For $\alpha = 1$ the two probabilities merge.

the inner horizon $r = r_-$. Obviously, the smaller α the smaller is the probability that a trapping surface occurs. Moreover, as we expected from the start, the density profiles coincide in the extremal case $\alpha = 1$ (thick and thin dashed lines), because the two horizons merge.

22 *R. Casadio, A. Giugno and O. Micu*

Integrating over r_{\pm} , we obtain the probabilities [§]

$$\begin{aligned}
 P_{\text{BH}\pm}(\ell, \alpha) = & \operatorname{erf} \left[\frac{\ell_{\text{p}}^2}{\ell^2} \left(1 \pm \sqrt{1 - \alpha^2} \right) \right] + \frac{\sqrt{\pi}}{2} \frac{\operatorname{erfc} \left[\frac{\ell_{\text{p}}^2}{\ell^2} \left(1 \pm \sqrt{1 - \alpha^2} \right) \right]}{\Gamma \left(\frac{3}{2}, 1 \right)} \\
 & - \frac{\left(1 \pm \sqrt{1 - \alpha^2} \right) \ell_{\text{p}}^2 / \ell^2}{\sqrt{\pi} \Gamma \left(\frac{3}{2}, 1 \right)} \frac{3 + \frac{\ell_{\text{p}}^4}{\ell^4} \left(1 \pm \sqrt{1 - \alpha^2} \right)^2}{\left[1 + \frac{\ell_{\text{p}}^4}{\ell^4} \left(1 \pm \sqrt{1 - \alpha^2} \right)^2 \right]^2} e^{-\left[1 + \left(1 \pm \sqrt{1 - \alpha^2} \right)^2 \frac{\ell_{\text{p}}^4}{\ell^4} \right]} \\
 & - \frac{2\sqrt{\pi}}{\Gamma \left(\frac{3}{2}, 1 \right)} T \left[\sqrt{2} \frac{\ell_{\text{p}}^2}{\ell^2} \left(1 \pm \sqrt{1 - \alpha^2} \right), \frac{\ell^2}{\ell_{\text{p}}^2 \left(1 \pm \sqrt{1 - \alpha^2} \right)} \right]. \quad (63)
 \end{aligned}$$

where T is again the Owen's function (A.7).

Fig. 11 shows how these probabilities vary with the parameter α for values of ℓ above or below the Planck scale. For the outer horizon, it is clear that $P_{\text{BH}+} \simeq 1$ for widths $\ell \lesssim \ell_{\text{p}}$ (mass larger than m_{p}). On the contrary, when $\ell \gtrsim \ell_{\text{p}}$ (or $m \lesssim m_{\text{p}}$), the probability sensibly decreases as the specific charge α approaches 1 from below. We see that this probability does not exactly vanish even when ℓ exceeds the Planck length ℓ_{p} . As an example, for $\ell = 2\ell_{\text{p}}$, corresponding to $m = m_{\text{p}}/2$, we find $0.15 \lesssim P_{\text{BH}+}(\alpha) \lesssim 0.2$ for a large interval of values of the specific charge. $P_{\text{BH}+}$ only falls below 0.1 right before the BH becomes maximally charged ($\alpha \simeq 1$). As far as the inner horizon is concerned, the scenario is profoundly different. The same plot shows that the probability $P_{\text{BH}-} \ll 1$ for small values of α and increases with this parameter. However, the role of ℓ is prominent because the sharper the Gaussian packet is localised in space (or the more massive it is), the smaller the value of α for which this probability becomes significant. To summarise, there is an appreciable range of values of the specific charge α for which the inner horizon is not likely to exist ($P_{\text{BH}-} \ll 1$), while the system is a BH ($P_{\text{BH}+} \simeq 1$).

The probabilities $P_{\text{BH}\pm}$ as functions of the width ℓ are shown in Fig. 12 and as functions of the mass m in Fig. 13, for $\alpha = 0.3, 0.8$ and 1 . It is evident that smaller values of α allow for $P_{\text{BH}+}$ to approach 1 for smaller masses m . The specular situation happens when studying the inner probability $P_{\text{BH}-}$. If we focus on the smallest specific charge considered here, $\alpha = 0.3$, we notice that both probabilities are close to 1 only around $m \simeq 6m_{\text{p}}$, and not at the naively expected scale $m \simeq m_{\text{p}}$. Hence, there exists a non-negligible interval in the possible values of m (around the Planck scale) for $\alpha < 1$ in which

$$P_{\text{BH}+} \simeq 1 \quad \text{and} \quad P_{\text{BH}-} \ll 1. \quad (64)$$

In this interval, the system is most likely a BH, because it is the outer horizon which dictates this property, while the inner horizon is still not very likely to exist. Lowering the value of α this range grows larger, while it narrows and eventually vanishes when approaching the maximally charged limit $\alpha = 1$.

[§]It is convenient to define $x_{\pm} = \ell r_{\pm} / \ell_{\text{p}}^2 (1 \pm \sqrt{1 - \alpha^2})$, and use again Eq. (A.8), with $A = (1 \pm \sqrt{1 - \alpha^2}) \ell_{\text{p}}^2 / \ell^2$.

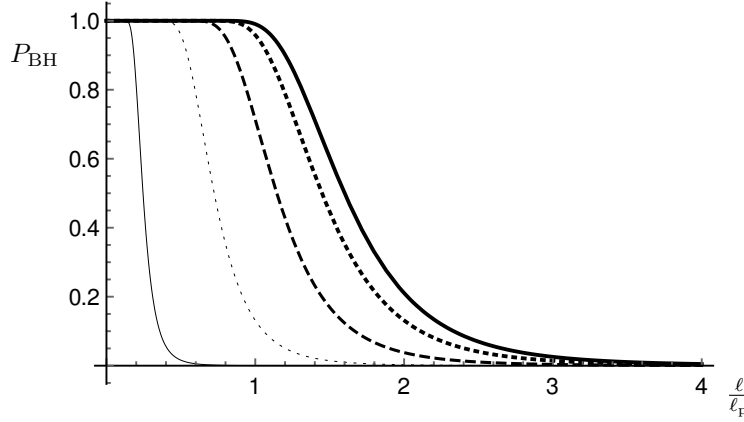


Fig. 12. Probability $P_{\text{BH}+}$ for the particle to be a BH (thick lines) and $P_{\text{BH}-}$ for the particle to be inside its inner horizon (thin lines), in Eq. (63), as functions of ℓ , for $\alpha = 0.3$ (continuous line), $\alpha = 0.8$ (dotted line) and $\alpha = 1$ (dashed line). For $\alpha = 1$ thick and thin dashed lines overlap.

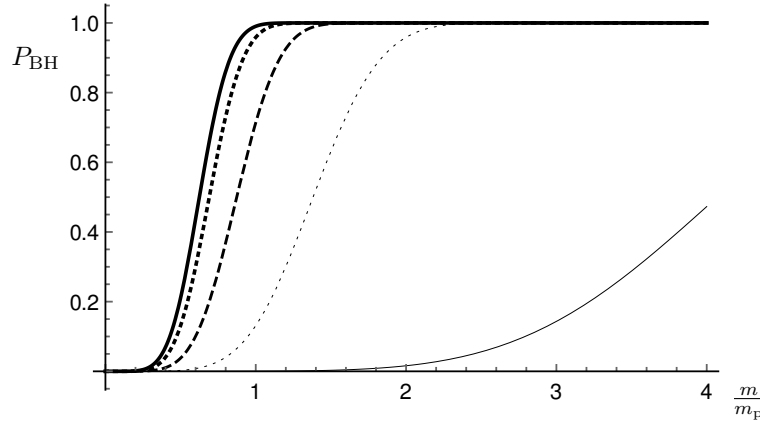


Fig. 13. Probability $P_{\text{BH}+}$ for the particle to be a BH (thick lines) and $P_{\text{BH}-}$ for the particle to be inside its inner horizon (thin lines), in Eq. (63), as functions of m , for $\alpha = 0.3$ (continuous line), $\alpha = 0.8$ (dotted line) and $\alpha = 1$ (dashed line). For $\alpha = 1$ thick and thin dashed lines overlap.

We conclude by remarking that we could have guessed this result. In fact, the smaller α , the more the system looks like a neutral (Schwarzschild) BH, since the mass becomes the dominant parameter and the presence of charge is (at most) a small perturbation. However, the existence of an inner horizon at $r = R_-$ is phenomenologically very important, because of the possible instability known as *mass inflation*^{97–99} related to the specific features of such a Cauchy horizon. Eq. (64) suggests that this instability should not always occur for $0 < \alpha \leq 1$, even when the particle is (most likely) a BH.

24 *R. Casadio, A. Giugno and O. Micu*

3.2.2. Quantum Cosmic Censorship

Overcharged sources with $\alpha > 1$ were analysed in Ref.⁴⁵ We recall that the cosmic censorship¹⁴ was conjectured in order to exclude such naked singularities from General Relativity. It is therefore interesting to investigate whether quantum physics supports this view or can introduce modifications of any kind. The analysis is developed by assuming that the overcharged regime $\alpha > 1$ is reached by continuing analytically the HWF from the case $0 < \alpha \leq 1$. It is clear that this choice is again not unique, but it should be consistent at least when the specific charge is not much greater than the classical limiting threshold $\alpha = 1$.

The first issue that needs to be taken into consideration for $\alpha > 1$ is that the operators \hat{r}_{\pm} directly obtained from Eq. (59) are not Hermitian. This could in principle be a reason to give up any observables corresponding to \hat{r}_{\pm} in this classically forbidden region. Nonetheless, one can follow through and construct a Hermitian radial operator using only the real parts of the multiplicative operators \hat{r}_{\pm} . By continuing analytically Eq. (60) for $\alpha > 1$, the square modulus of the HWF becomes⁴⁵

$$|\psi_{\text{H}}(r_{\text{H}})|^2 = \mathcal{N}^2 \exp \left\{ -\frac{2 - \alpha^2}{\alpha^4} \frac{\ell^2 r_{\text{H}}^2}{\ell_{\text{p}}^4} \right\}, \quad (65)$$

where r_{H} now replaces both r_+ and r_- (which in fact merge at $\alpha = 1$) and \mathcal{N} is a normalisation factor. It so happens that this HWF is still normalisable in the Schrödinger scalar product (16) if r_{H} is a real variable and for specific charge values in the range

$$1 < \alpha^2 < 2. \quad (66)$$

This suggests that there must be a quantum obstruction forbidding the system from crossing $\alpha^2 = 2$. We will discuss this issue more completely after determining the full HWF.

One also needs to modify the step function in Eq. (60) when the system enters the overcharged regime. First, we note that the real part of the complex Eq. (61) is the same for r_+ and r_- , and set

$$R_{\text{H}} = \text{Re} \left[\frac{\ell_{\text{p}}^2}{\ell} \left(1 \pm \sqrt{1 - \alpha^2} \right) \right] = \frac{\ell_{\text{p}}^2}{\ell}. \quad (67)$$

We can then show that the continuity property which leads to Eq. (65) extends to \hat{r}_{H} when r_{H} is bounded from below by R_{H} . In fact, we can compute the expectation value

$$\langle \hat{r}_{\text{H}} \rangle = 4\pi \int_{R_{\text{H}}}^{\infty} |\psi_{\text{H}}(r_{\text{H}})|^2 r_{\text{H}}^3 dr_{\text{H}} = \frac{\alpha^2}{\sqrt{2 - \alpha^2}} \frac{\Gamma\left(2, \frac{2 - \alpha^2}{\alpha^4}\right)}{\Gamma\left(\frac{3}{2}, \frac{2 - \alpha^2}{\alpha^4}\right)} R_{\text{H}}, \quad (68)$$

and observe that this expression matches the analogous expressions from the regime

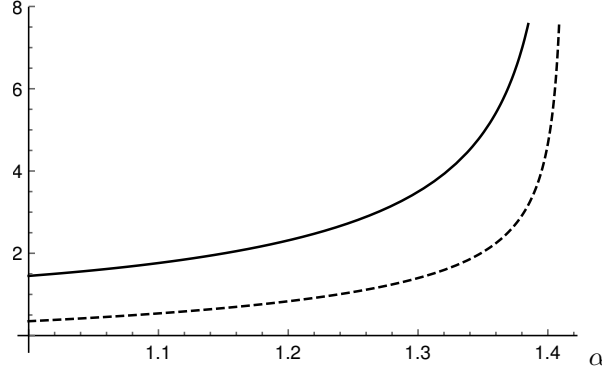


Fig. 14. Expectation value $\langle \hat{r}_H \rangle$ (solid line) and its uncertainty Δr_H (dashed line), in units of ℓ_P , as functions of the specific charge $1 < \alpha^2 < 2$ and $\ell = \ell_P$ ($m = m_p$).

$0 < \alpha \leq 1$,

$$\langle \hat{r}_\pm \rangle = 4\pi \int_{R_\pm}^{\infty} |\psi_\pm(r_\pm)|^2 r_\pm^3 dr_\pm = \frac{\Gamma(2,1)}{\Gamma(\frac{3}{2},1)} R_\pm, \quad (69)$$

in the limit $\alpha = 1$, namely

$$\lim_{\alpha \searrow 1} \langle \hat{r}_H \rangle = \frac{\Gamma(2,1)}{\Gamma(\frac{3}{2},1)} \frac{\ell_P^2}{\ell} = \lim_{\alpha \nearrow 1} \langle \hat{r}_\pm \rangle. \quad (70)$$

Moreover, the same holds for the corresponding uncertainties, that is

$$\Delta r_H^2(\ell, \alpha \rightarrow 1^+) = \Delta r_\pm^2(\ell, \alpha \rightarrow 1^-). \quad (71)$$

We omit the details here,⁴⁵ and just remark that, for $\alpha = 1$, the width of the Gaussian $\ell > \langle \hat{r}_H \rangle$ for $m < \sqrt{\Gamma(\frac{3}{2},1)/\Gamma(2,1)} m_p \simeq 0.8 m_p$. The gravitational fluctuations in the size of the source will thus be subdominant when its mass is sensibly smaller than the Planck mass m_p , like in the neutral case.

Let us now consider what happens when approaching the critical specific charge $\alpha^2 = 2$. One may have already noticed that

$$\langle \hat{r}_H \rangle \simeq \frac{8}{\sqrt{\pi(2-\alpha^2)}} \frac{\ell_P^2}{\ell}, \quad (72)$$

so that the ratio $\langle \hat{r}_H \rangle/\ell$ diverges in the limit $\alpha^2 \rightarrow 2$, regardless of the mass $m = m_p \ell_P/\ell$. Moreover, since

$$\Delta r_H \simeq \sqrt{3\pi/8-1} \langle \hat{r}_H \rangle \simeq 0.4 \langle \hat{r}_H \rangle, \quad (73)$$

the uncertainty Δr_H shows the same behaviour for $\alpha^2 \rightarrow 2$ (see also Fig. 14).

In the same way that led to Eq. (63), we can obtain the probability P_{BH} that the particle is a BH for α in the allowed range (66),

$$P_{\text{BH}} = \frac{4}{\sqrt{\pi} \Gamma(\frac{3}{2}, \frac{2-\alpha^2}{\alpha^4})} \int_{\frac{\sqrt{2-\alpha^2}}{\alpha^2}}^{\infty} \gamma\left(\frac{3}{2}, \frac{\alpha^4}{2-\alpha^2} \frac{\ell_P^4}{\ell^4} x^2\right) e^{-x^2} x^2 dx, \quad (74)$$

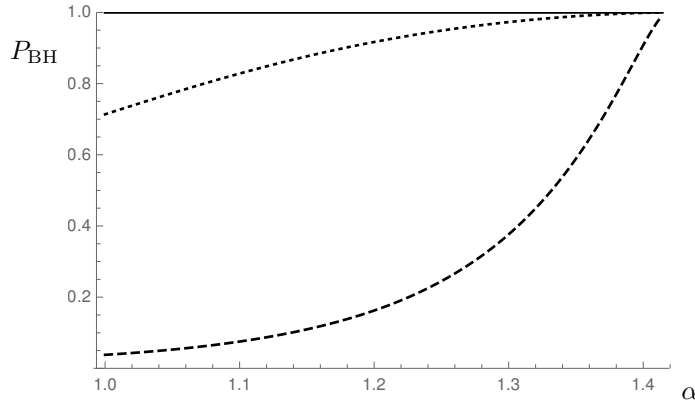


Fig. 15. P_{BH} as a function of α for $\ell = \ell_{\text{p}}/2$ (solid line), $\ell = \ell_{\text{p}}$ (dotted line) and $\ell = 2\ell_{\text{p}}$ (dashed line). Cases with $\ell \ll \ell_{\text{p}}$ are not plotted since they behave the same as $\ell = \ell_{\text{p}}/2$, i.e. an object with $1 < \alpha^2 < 2$ must be a BH.

where $x \equiv \sqrt{2 - \alpha^2} \ell r_{\text{H}} / \alpha^2 \ell_{\text{p}}^2$.

This probability is computed numerically and plotted in Fig. 15 as a function of α . One notes that, for a Gaussian width much smaller than ℓ_{p} , $P_{\text{BH}} \simeq 1$ throughout the whole range of the specific charge, which extends a similar result for $0 < \alpha \leq 1$. Nevertheless, even when ℓ significantly exceeds the Planck length, we see that the same result is obtained in the limit $\alpha^2 \rightarrow 2$. It is important to recall that, when the system is far from the Planck scale, $\ell \gg \langle \hat{r}_{\text{H}} \rangle$, quantum fluctuations in the particle's position dominate and $P_{\text{BH}} \ll 1$ accordingly. However, strong quantum fluctuations in the size of the horizon appear in the overcharged regime where the probability P_{BH} is large, since $\langle \hat{r}_{\text{H}} \rangle$ and Δr_{H} blow up for $\alpha^2 \rightarrow 2$.

Bearing all the limitations and ambiguities in the above analysis, the picture that emerges is that of a *quantum* version of the cosmic censorship: first of all it appears that (slightly) overcharged configurations may exist, but have a large probability of being BHs, rather than naked singularities; secondly, when the specific charge is larger than a critical value (here found to be $\alpha \simeq 1.4$), there exist no well-behaved HWF and the gravitational radius of the system cannot be defined. Of course, one should not forget that assuming a Gaussian wave-function for the source already restricts these conclusions to masses of the order of the Planck scale, and not too much larger, as we recalled in section 3.1.1.

3.3. Particle collisions in (1 + 1) dimensions

A straightforward extension of the HQM to a state containing two free particles colliding head-on in one-dimensional flat space was presented in Ref.,⁴⁶ where both constituents are represented by Gaussian wave-functions centred around the posi-

tions X_i and having linear momentum P_i ($i = 1$ or 2),

$$\langle x_i; 0 | \psi_S^{(i)} \rangle \equiv \psi_S(x_i) = e^{-i \frac{P_i x_i}{m_p \ell_p}} \frac{e^{-\frac{(x_i - X_i)^2}{2 \Delta_i}}}{\sqrt{\pi^{1/2} \Delta_i}}, \quad (75)$$

where dynamical phases are neglected since we will only consider “snapshots” of the collision. Like in the one-particle case, one switches to momentum space in order to compute the spectral decomposition of the system,

$$\langle p_i; 0 | \psi_S^{(i)} \rangle \equiv \psi_S(p_i) = e^{-i \frac{p_i X_i}{m_p \ell_p}} \frac{e^{-\frac{(p_i - P_i)^2}{2 \Delta_i}}}{\sqrt{\pi^{1/2} \Delta_i}}, \quad (76)$$

where the width $\Delta_i = m_p \ell_p / \ell_i$, and we will use the relativistic flat-space dispersion relation $E_i^2 = p_i^2 + m_i^2$, just like in the single particle case (25). It is particularly interesting to consider particles with masses $m_1 \simeq m_2 \ll m_p$, so that the probability that they form a BH can be significant only in the ultra-relativistic limit $|P_i| \sim E_i \sim m_p$, which implies

$$\ell_i \simeq \frac{\ell_p m_p}{|P_i|}, \quad \Delta_i \simeq |P_i|. \quad (77)$$

The two-particle state can be written as

$$| \psi_S^{(1,2)} \rangle = \prod_{i=1}^2 \left[\int_{-\infty}^{+\infty} dp_i \psi_S(p_i, t) | p_i \rangle \right], \quad (78)$$

and the coefficients in the spectral decomposition (12) are given by

$$C(E) = \int_{-\infty}^{+\infty} \int_{-\infty}^{+\infty} \psi_S(p_1) \psi_S(p_2) \delta(E - E_1 - E_2) dp_1 dp_2. \quad (79)$$

The HWF is defined in the rest frame of the possible BH, that is in the centre-of-mass coordinate system with $P_1 = -P_2 \equiv P > 0$. From $P \sim m_p \gg m_1 \simeq m_2$, we can also set $X_1 \simeq -X_2 \equiv X > 0$. The unnormalised HWF is then given by⁴⁶

$$\begin{aligned} \psi_H = & e^{-\frac{m_p r_H^2}{16 \ell_p^2 P} - \frac{X^2 P^2}{\ell_p^2 m_p^2}} \text{Erf} \left(1 + \frac{m_p r_H}{4 \ell_p P} + i \frac{XP}{\ell_p m_p} \right) \\ & - e^{-\frac{m_p r_H^2}{16 \ell_p^2 P} - \frac{X^2 P^2}{\ell_p^2 m_p^2}} \text{Erf} \left(1 - \frac{m_p r_H}{4 \ell_p P} - i \frac{XP}{\ell_p m_p} \right) \\ & + 2 e^{-1 - \frac{2iXP}{\ell_p m_p} - \frac{m_p r_H^2}{16 \ell_p^2 P}} \cosh \left(\frac{m_p r_H}{2 \ell_p P} + i \frac{r_H X}{2 \ell_p^2} \right) \text{Erf} \left(\frac{m_p r_H}{4 \ell_p P} \right), \quad (80) \end{aligned}$$

whose normalisation can be computed numerically for fixed X and P .

The energy of the system is solely determined by the momentum, and in fact we notice from Fig. 16 that $\mathcal{P}_H = |\psi_H(r_H)|^2$ does not vary much with X , but is clearly affected by P (see Fig. 17). Moreover, the peak of the probability density \mathcal{P}_H is always located around $r_H \simeq 2 \ell_p (2P/m_p)$.

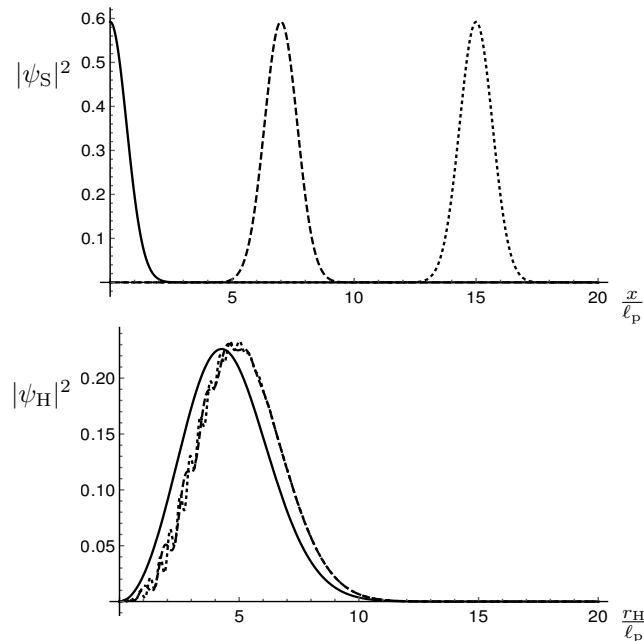


Fig. 16. Top panel: square modulus of ψ_S for $P = m_p$ and $X = 0$ (solid line) $X = 7 \ell_p$ (dashed line) and $X = 15 \ell_p$ (dotted line). Bottom panel: square modulus of ψ_H for $P = m_p$ and $X = 0$ (solid line) $X = 7 \ell_p$ (dashed line) and $X = 15 \ell_p$ (dotted line). Particles are inside the horizon only for sufficiently small X .

The final step is to compute the probability (20) that the two-particle system is a BH as a function of the distance X of each particle from the center-of-mass and the total energy $2P$ (see Fig. 18). One may argue that a rough estimate of the time evolution is given by considering this function along lines of constant P and decreasing X . In fact, it is easy to see that the probability increases to a maximum for $X = 0$, when the two particles overlap exactly. Hence, there is a large probability that the collision forms a BH, e.g. $P_{\text{BH}}(X, 2P \gtrsim 2m_p) \gtrsim 80\%$, when

$$X \lesssim 2 \ell_p (2P/m_p) - \ell_p = r_{\text{H}}(2P) - \ell_p. \quad (81)$$

The second term in the r.h.s. can be viewed as a quantum correction to the hoop formula (1) for $E \simeq 2P \gtrsim 2m_p$, and becomes negligible for large (semi)classical BHs produced in collisions with $2P \gg m_p$. Lowering P , we have that the region $P_{\text{BH}}(X, 2P \lesssim 2m_p) \gtrsim 80\%$ corresponds to the momenta satisfying $2P \gtrsim m_p (1 + X^2/9 \ell_p^2)$ and its boundary $P_{\text{BH}}(X, 2P \lesssim 2m_p) \simeq 80\%$ can be approximated by

$$2P - m_p \simeq m_p X^2/9 \ell_p^2, \quad (82)$$

which crosses the axis $X = 0$ for $2P \simeq m_p$. This curve represents a further correction to the hoop conjecture (1), and supports the conclusion that the mass of quantum BHs is bounded below by about m_p . We should remark that, although these numerical values strongly depend on what probability P_{BH} is considered large

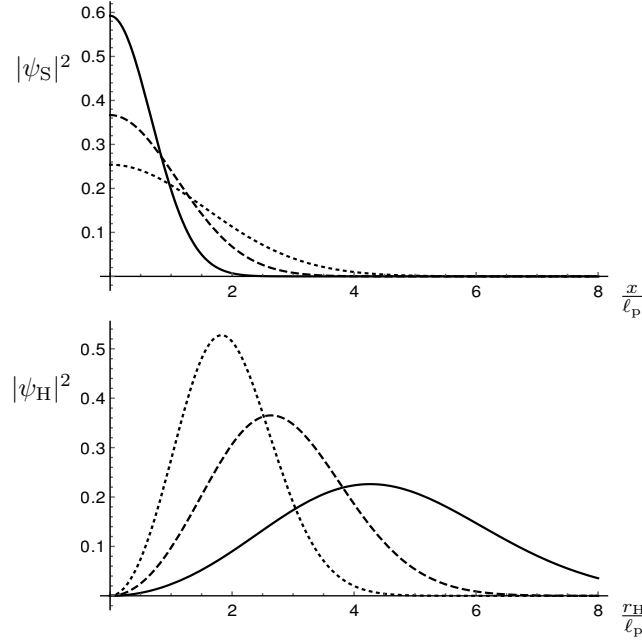


Fig. 17. Top panel: square modulus of ψ_S for $X = 0$ and $P = m_p$ (solid line) $P = 3 m_p/5$ (dashed line) and $P = 2 m_p/5$ (dotted line). Bottom panel: square modulus of ψ_H for $X = 0$ and $P = m_p$ (solid line) $P = 3 m_p/5$ (dashed line) and $P = 2 m_p/5$ (dotted line). Particles' location is sharper the fuzzier (more spread) the horizon location and vice versa.

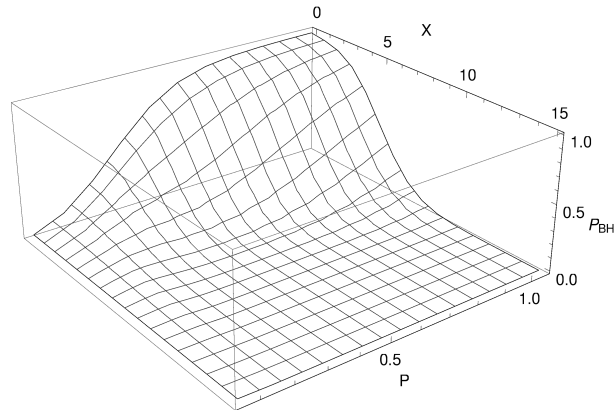


Fig. 18. Probability the two-particle system is a BH as a function of X and P (in units of Planck length and mass respectively).

enough, the slope in Eq. (81) agrees perfectly with Eq. (1). One can thus conclude that, despite the great simplifications assumed in this analysis, the HQM appears

suitable to extend the hoop conjecture into the quantum description of BH formation.

3.4. Higher and lower dimensional models

The idea that the number of dimensions of space-time is not exactly four as we experience, was proposed in order to explain some puzzles of the Standard Model, like the hierarchy problem, or for consistence with string theory. Remarkably, in $D > 3$ spatial dimensions, the fundamental gravitational mass $m_D \ll m_p$, and $\ell_D = \hbar/m_D \gg \ell_p$, where

$$G_D = \frac{\ell_D^{D-2}}{m_D} . \quad (83)$$

This opens up the possibility of having much lighter BHs, possibly within the reach of current high-energy experiments.^{100,101} This happens both in the ADD^{102,103} and the Randall-Sundrum^{104,105} models (for a comprehensive, see Ref.¹⁰⁶). In Ref.⁴³ the HQM probability that BHs form in the ADD scenario was computed, with some interesting consequences.

It is also instructive to study theories with less than three spatial dimensions, since the corresponding quantum theories are simpler and can be solved exactly.¹⁰⁷ In recent years, interest in such theories was also revived by the possibility that the number of spatial dimensions effectively decreases when approaching ℓ_p , regardless of the model under consideration. This effect is called “spontaneous dimensional reduction” and has been extended to various contexts, most of which with special focus on the energy dependence of the spectral dimension, including causal dynamical triangulations^{108–110} and non-commutative geometry inspired mechanisms.^{111–114} An alternative approach is built on the claim that the effective dimensionality of space-time increases as the ambient energy scale decreases.^{115–120}

3.4.1. $(1 + D)$ -dimensional Schwarzschild metric

In D spatial dimensions, the generalised Schwarzschild metric is given by

$$ds^2 = - \left(1 - \frac{R_D}{r^{D-2}} \right) dt^2 + \left(1 - \frac{R_D}{r^{D-2}} \right)^{-1} dr^2 + r^{D-1} d\Omega_{D-1} , \quad (84)$$

where the classical horizon radius is

$$R_D = \left(\frac{2 G_D m}{|D-2|} \right)^{\frac{1}{D-2}} = \begin{cases} \frac{1}{2 G_1 m} & \text{if } D = 1 \\ \left(\frac{2 G_D m}{D-2} \right)^{\frac{1}{D-2}} & \text{if } D > 2 . \end{cases} \quad (85)$$

Note that $D = 2$ is excluded because in that case there exists no asymptotically flat BH, and we do not want to include a cosmological constant.

The source of the gravitational field is still described by a Gaussian wavefunction, that is

$$\psi_S(r) = \frac{e^{-\frac{r^2}{2\ell^2}}}{(\ell\sqrt{\pi})^{D/2}}, \quad (86)$$

whose momentum space counterpart is

$$\tilde{\psi}_S(p) = \frac{e^{-\frac{p^2}{2\Delta^2}}}{(\Delta\sqrt{\pi})^{D/2}}, \quad (87)$$

where $\Delta = m_D \ell_D / \ell$ and, taking again Eq. (22), $\ell \sim m^{-1}$, we recover $\Delta \simeq m$. As in $D = 3$, we assume the relativistic mass-shell relation in flat space (25), and, for $D > 3$, one obtains the HWF

$$\begin{aligned} \psi_H = & \left\{ \frac{D-2}{\ell_D^D \pi^{D/2}} \left[\frac{(D-2)\ell}{2\ell_D} \right]^{\frac{D}{D-2}} \frac{\Gamma\left(\frac{D}{2}\right)}{\Gamma\left(\frac{D}{2D-4}, 1\right)} \right\}^{1/2} \\ & \times \Theta(r_H - R_D) \exp \left\{ -\frac{(D-2)^2}{8} \frac{\ell^2 r_H^{2(D-2)}}{\ell_D^{2(D-1)}} \right\}, \end{aligned} \quad (88)$$

whose normalisation was fixed in the scalar product

$$\langle \psi_H | \phi_H \rangle = \Omega_{D-1} \int_0^\infty \psi_H^*(r_H) \phi_H(r_H) r_H^{D-1} dr_H, \quad (89)$$

where Ω_{D-1} is the volume of the D -sphere.

For $D = 1$, there is an important change of sign in the argument of the step function. In fact, the generalisation (8) of the hoop conjecture (1) is now satisfied when $0 \leq r_H \leq R_1$ and the HWF reads

$$\psi_H = \sqrt{\frac{2/\ell}{\Gamma\left(-\frac{1}{2}, 1\right)}} \Theta(R_1 - r_H) \exp \left\{ -\frac{\ell^2}{8r_H^2} \right\}, \quad (90)$$

which otherwise is the same as (88) with $D = 1$.

3.4.2. BH probability

It is straightforward to write down the probability for the particle to be inside a D -dimensional ball of radius r_H ,

$$P_S(r < r_H) = \Omega_{D-1} \int_0^{r_H} |\psi_S(r)|^2 r^{D-1} dr, \quad (91)$$

and the probability density that the gravitational radius equals r_H is

$$\mathcal{P}_H(r_H) = \Omega_{D-1} r_H^{D-1} |\psi_H(r_H)|^2. \quad (92)$$

32 *R. Casadio, A. Giugno and O. Micu*

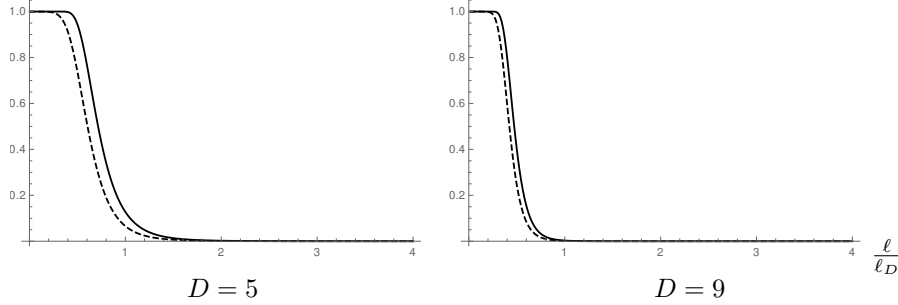


Fig. 19. Probability $P_{\text{BH}}(\ell)$ of a particle to be a BH (straight line) compared to its analytical approximation (dashed line), for $D = 5$ and 9.

Omitting the details, one then finds

$$\begin{aligned} \mathcal{P}_< &= \frac{2}{\ell_D^D} \left[\frac{(D-2)\ell}{2\ell_D} \right]^{\frac{D}{D-2}} \frac{D-2}{\Gamma\left(\frac{D}{2D-4}, 1\right) \Gamma\left(\frac{D}{2}\right)} \Theta(r_{\text{H}} - R_D) \\ &\times \gamma\left(\frac{D}{2}, \frac{r_{\text{H}}^2}{\ell^2}\right) \exp\left\{-\frac{(D-2)^2}{4} \frac{\ell^2 r_{\text{H}}^{2(D-2)}}{\ell_D^{2(D-1)}}\right\} r_{\text{H}}^{D-1} \end{aligned} \quad (93)$$

and the BH probability is

$$\begin{aligned} P_{\text{BH}} &= \frac{2(D-2)}{\Gamma\left(\frac{D}{2D-4}, 1\right) \Gamma\left(\frac{D}{2}\right)} \\ &\times \int_1^\infty \gamma\left(\frac{D}{2}, \left[\frac{2}{D-2} \left(\frac{\ell_D}{\ell}\right)^{D-1}\right]^{\frac{2}{D-2}} x_D^2\right) e^{-x_D^{2(D-2)}} x_D^{D-1} dx_D, \end{aligned} \quad (94)$$

where we defined $x_D^{D-2} = (D-2)\ell r_{\text{H}}^{D-2}/2\ell_D^{D-1}$. Eq. (94) depends, as usual, on the Gaussian width ℓ , but also on the number D of spatial dimensions (with $D = 3$ reproducing Eq. (29)). Since the above integral cannot be performed analytically for a general D , in Fig. 19 we show the numerical dependence on ℓ of the above probability for different spatial dimensions, and compare it with the approximation obtained by taking the limit $R_D \rightarrow 0$.

The most important fact here is that the probability $P_{\text{BH}} = P_{\text{BH}}(m, D)$ at a given m decreases significantly for increasing D , and for large values of D a particle of mass $m \simeq m_D$ is most likely not a BH. This result should have a strong impact on the number of BHs produced in particle collisions. In fact, one expects the effective production cross-section $\sigma(E) \sim P_{\text{BH}}(E) \sigma_{\text{BH}}(E)$, where $\sigma_{\text{BH}} \sim 4\pi E^2$ is the usual expression following from Eq. (1). Since P_{BH} can be very small, $\sigma(E) \ll \sigma_{\text{BH}}(E)$ for $D > 4$, and much less BHs should be produced than estimated previously.¹⁰¹

For $D = 1$ and $\ell = \lambda_m$, we can integrate the density

$$P_{\text{H}} = \frac{2/\ell}{\Gamma\left(-\frac{1}{2}, 1\right)} \Theta(R_1 - |r_{\text{H}}|) \text{erf}\left(\frac{r_{\text{H}}}{\ell}\right) \exp\left\{-\frac{\ell^2}{4r_{\text{H}}^2}\right\}, \quad (95)$$

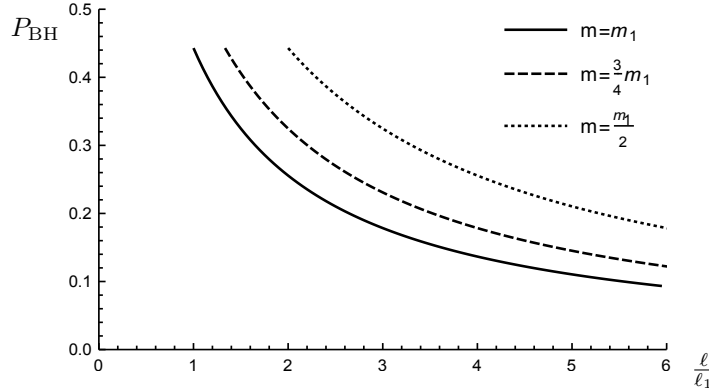


Fig. 20. Probability $P_{\text{BH}}(\ell, m)$ for a particle to be a BH in $D = 1$, for $m = m_1$ (solid line), $m = 3m_1/4$ (dashed line) and $m = m_1/2$ (dotted line).

obtained from Eq. (90), and find

$$P_{\text{BH}} = \frac{1}{\Gamma(-\frac{1}{2}, 1)} \int_0^1 \text{erf}\left(\frac{x_1}{2}\right) e^{-\frac{1}{x_1^2}} dx_1 \simeq 0.44, \quad (96)$$

where $x_1 = 2r_{\text{H}}/\ell$, which can also be obtained from Eq. (94) by setting $D = 1$. This last equation reveals a striking difference between $D = 1$ and higher-dimensional space-times. The maximum probability that a BH may form is independent of the mass of the source. This result is supported by the fact that the one-dimensional gravitational constant $G_1 = \hbar$ and

$$\langle \hat{r}_{\text{H}} \rangle \simeq R_1(m) \simeq \lambda_m, \quad (97)$$

for any possible mass, and hence no source can be treated in a classical way. Moreover, for more general cases with $\ell > \lambda_m$, particles with masses considerably lower than the mass scale m_1 still have a relatively large probability to be BHs (see Fig. 20).⁴³ Another important feature of the HWF in $D = 1$ is that

$$\Delta r_{\text{H}} \simeq \ell \simeq \Delta p^{-1}, \quad (98)$$

that is the uncertainty in the horizon radius shows the same dependence on the momentum uncertainty found in the Heisenberg relation. This implies that we cannot obtain a GUP in $D = 1$ by combining (linearly) the above the two uncertainties, unlike in the three-dimensional case (38). In fact, all of these results agree with the notion that two-dimensional BHs are strictly quantum objects.¹¹⁴

3.4.3. GUP from HWF in higher dimensions

For $D > 3$, we have

$$\langle \hat{r} \rangle = \frac{2^{1-D} \sqrt{\pi} (D-1)!}{\Gamma(\frac{D}{2})^2} \ell \quad (99)$$

34 *R. Casadio, A. Giugno and O. Micu*

and

$$\langle \hat{r}^2 \rangle = \frac{D}{2} \ell^2 . \quad (100)$$

Moreover,

$$\Delta p = \sqrt{A_D} m = \sqrt{A_D} m_D \frac{\ell_D}{\ell} , \quad (101)$$

so that

$$\frac{\Delta r}{\ell_D} = \sqrt{A_D} \frac{\ell}{\ell_D} = A_D \frac{m_D}{\Delta p} , \quad (102)$$

where

$$A_D \equiv \frac{D}{2} - \left(\frac{2^{1-D} \sqrt{\pi}}{\Gamma\left(\frac{D}{2}\right)^2} (D-1)! \right)^2 . \quad (103)$$

From the HWF (88), we likewise obtain the expectation values

$$\langle \hat{r}_H \rangle = \frac{\mathbb{E}_{\frac{D-5}{2D-4}}(1)}{\mathbb{E}_{\frac{D-4}{2D-4}}(1)} R_D \quad (104)$$

and

$$\langle \hat{r}_H^2 \rangle = \frac{\mathbb{E}_{\frac{D-6}{2D-4}}(1)}{\mathbb{E}_{\frac{D-4}{2D-4}}(1)} R_D^2 , \quad (105)$$

in terms of the exponential integral (36), so that

$$\frac{\Delta r_H}{\ell_D} = C_D \left(\frac{\ell_D}{\ell} \right)^{\frac{1}{D-2}} = B_D \left(\frac{\Delta p}{m_D} \right)^{\frac{1}{D-2}} , \quad (106)$$

where $B_D = A_D^{-\frac{2}{D-2}} C_D$ and

$$C_D = \sqrt{\frac{\mathbb{E}_{\frac{D-6}{2D-4}}(1)}{\mathbb{E}_{\frac{D-4}{2D-4}}(1)} - \left(\frac{\mathbb{E}_{\frac{D-5}{2D-4}}(1)}{\mathbb{E}_{\frac{D-4}{2D-4}}(1)} \right)^2} \left(\frac{2}{D-2} \right)^{\frac{1}{D-2}} . \quad (107)$$

By combining the two uncertainties (102) and (106) linearly, one finally finds

$$\frac{\Delta r}{\ell_D} = A_D \frac{m_D}{\Delta p} + \xi B_D \left(\frac{\Delta p}{m_D} \right)^{\frac{1}{D-2}} , \quad (108)$$

where, like before, the coefficient ξ is a dimensionless parameter.

Fig. 21 shows the total uncertainty Δr for different numbers of spatial dimensions (and $\xi = 1$). It is clear that in higher dimensions, one obtains the same qualitative behaviour as in $D = 3$, with Eq. (108) being again minimised by a length L_D corresponding to an energy scale M_D , which we plot in Figs. 22 and 23 as functions of the parameter ξ . From these plots we can infer that, for every value of D considered here, the assumption $M_D \simeq m_D$ makes large values of ξ significant, whilst the opposite happens if we set $L_D \simeq \ell_D$.

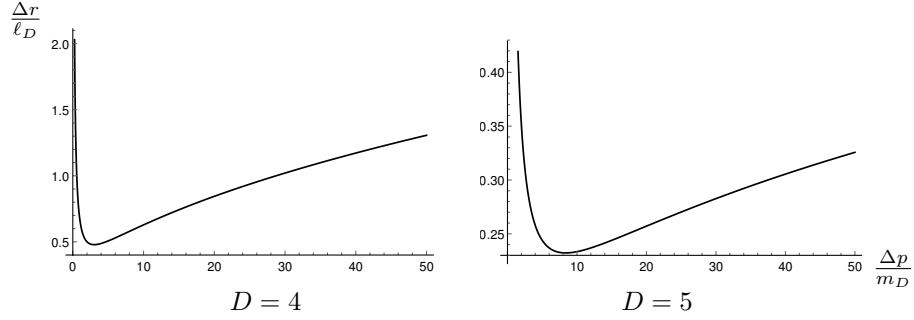


Fig. 21. Uncertainty Δr as function of Δp for $D = 4$ and 5 and $\xi = 1$.

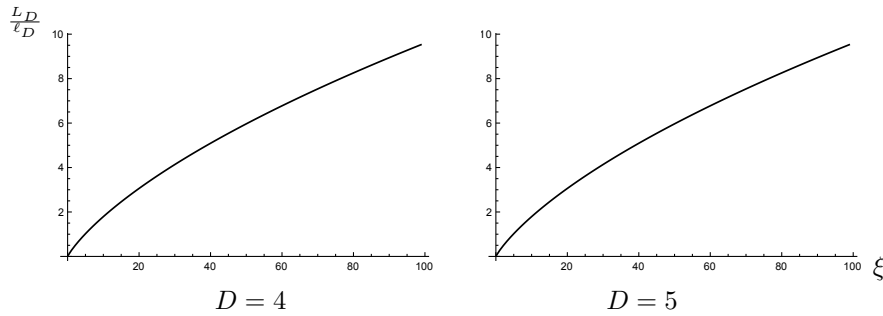


Fig. 22. Minimum scale L_D as function of the parameter ξ for $D = 4$ and 5 .

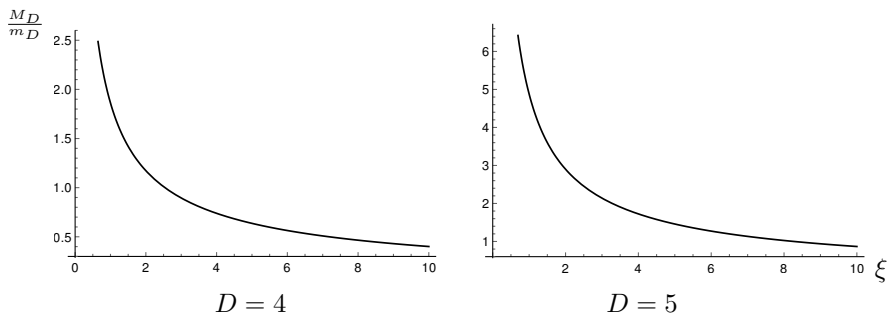


Fig. 23. Minimum scale M_D as function of the parameter ξ for $D = 4$ and 5 .

4. Causal time evolution

So far, time evolution was not considered. In the case of the two colliding wave-packets, one could sort of infer how the probability for the system of particles to form a BH evolves by looking at the plot representing this probability as a function of the distance between the two particles. However, in this crude approximation, nothing would forbid the two particles from crossing each other, and the probability P_{BH} to reach one and then decrease. How a non-negligible BH probability could affect

36 *R. Casadio, A. Giugno and O. Micu*

the evolution of a quantum state was addressed in Ref.⁴² for the usual spherically symmetric Gaussian wave-packet (21). In order to simplify the analysis, all Standard Model interactions are neglected and the point of view is taken of an observer placed at a very large distance from this particle. It seems therefore sensible to assume that, if the particle is not a BH ($P_{\text{BH}} \ll 1$), the time evolution is governed by the standard Schrödinger equation with the Hamiltonian $H = E$ of the mass-shell Eq. (25). If instead the system is a BH ($P_{\text{BH}} \simeq 1$), no evolution should appear to occur at all (Hawking evaporation is also neglected in this toy model). The picture considered in Ref.⁴² is therefore of a BH as a “frozen star”^h.

When the wave-packet ψ_S does not fall into one of the above two limiting conditions, the evolution for arbitrarily “short” time intervals δt is taken to be described by means of the combination

$$\psi_S(r, t + \delta t) = \left[\mu_H(t) \hat{\mathbb{I}} + \bar{\mu}_H(t) e^{-\frac{i\delta t}{m_p \ell_p} \hat{H}} \right] \psi_S(r, t), \quad (109)$$

where $\hat{\mathbb{I}}$ is the identity operator and the coefficients

$$\mu_H(t) \simeq P_{\text{BH}}(t) \simeq 1 - \bar{\mu}_H(t), \quad (110)$$

so that the two limiting behaviours are included by construction and unitarity is preserved,

$$1 = \mu_H^2 + \bar{\mu}_H^2 + 2\bar{\mu}_H \mu_H \cos\left(\frac{\delta t}{m_p \ell_p} \hat{H}\right) \simeq (\mu_H + \bar{\mu}_H)^2, \quad (111)$$

for δt sufficiently short (see below about this very important point). In this limit, Eq. (109) results in the effective Schrödinger equation

$$i m_p \ell_p \frac{\delta \psi_S(r, t)}{\delta t} \simeq [1 - P_{\text{BH}}(t)] \hat{H} \psi_S(r, t), \quad (112)$$

which reproduces the standard quantum mechanical evolution in the limit $P_{\text{BH}} \rightarrow 0$. Since the (now time-dependent) probability $P_{\text{BH}} = P_{\text{BH}}(t)$ is determined by the entire wave-function $\psi_S = \psi_S(r, t)$ and its associated HWF, the apparently trivial correction it introduces is instead non-local, and cannot be reproduced by means of a local interaction term of the form $H_{\text{int}} = H_{\text{int}}(r, t)$. This insight makes it evident that it will be generally very hard to solve Eq. (112) for a finite time interval.

By employing the spectral decomposition at fixed time t ,

$$\psi_S(r, t) = \sum_E C_E(t) j_0(E, r), \quad (113)$$

where j_0 is a spherical Bessel function of the first kind, Eq. (109) can be written as

$$i m_p \ell_p \delta C_E(t) \simeq [1 - P_{\text{BH}}(t)] E C_E(t) \delta t. \quad (114)$$

^hHistorically, this name was commonly used for gravitationally collapsed objects before the term BH was introduced.⁵⁹

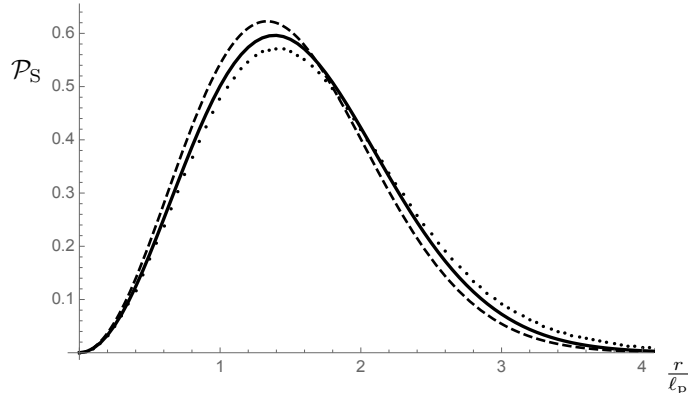


Fig. 24. Time-evolution of the probability density for the initial Gaussian packet (21) with $m = 3 m_p/4$ and $\ell = \lambda_m = 4 \ell_p/3$ (dashed line) according to standard quantum mechanics (dotted line) compared to its causal evolution (112) (solid line) for $\delta t = \ell_p$.

One can now determine $\delta C_E(t)$ provided $\psi_S(t)$ is known, and reconstruct both ψ_S and ψ_H at the time $t + \delta t$, in order to proceed to the next time step.

If $\psi_S(r, t = 0)$ is the Gaussian wave-function (21), the corresponding $P_{\text{BH}}(t = 0) = P_{\text{BH}}(\ell, m)$ discussed in Section 3.1, and this state will likely be a BH only if $m \gtrsim m_p$ and $\ell \lesssim \ell_p$. In particular, by setting $E \simeq m_p$, we expect the evolution equation (114) holds for

$$\delta t \lesssim \ell_p \frac{m_p}{E} \simeq \ell_p, \quad (115)$$

and even shorter intervals for modes with energy $E \gg m_p$, which is a form of the natural duality ($E > m_p$) \Leftrightarrow ($\delta t < \ell_p$). One can now solve Eq. (114) with a time step satisfying (115), and subsequently obtain the wave-function $\psi_S(r, t = \delta t)$ by inverting the decomposition (113). Fig. 24 shows the probability density $\mathcal{P}_S = 4\pi r^2 |\psi_S(r, t)|^2$ at $t = 0$ and $t = \delta t = \ell_p$ for $m = 3 m_p/4$ and $\ell = \lambda_m = 4 \ell_p/3$. One can make a comparison with the density arising from the standard free evolution during the same interval of time $\delta t = \ell_p$. In this case, the initial state is characterised by the minimum gravitational radius $R_H = 1.5 \ell_p$ given in Eq. (8), the expectation value of the energy $\langle E \rangle \simeq 1.15 m_p$, the Schwarzschild radius $\langle \hat{r}_H \rangle \simeq 2.3 \ell_p$, and initial probability $P_{\text{BH}} \simeq 0.8$. One immediately notices that the modified evolution makes the packet more confined than the usual quantum mechanical one. However, since the packet will keep on spreading, it is reasonable to guess that $P_{\text{BH}}(t + \delta t) < P_{\text{BH}}(t)$, and the effect of the horizon will mitigate over time.

Longer time evolutions can be obtained by discretising the time as $t = n \delta t$, where n is a positive integer and the time step δt is bounded by (115) for all relevant energies E in the spectrum (113). In Ref.⁴² a numerical approach was employed in order to keep all these features under control. Fig. 25 shows the probability densities \mathcal{P}_S and \mathcal{P}_H for $m = 3 m_p/4$ and $\ell = \lambda_m = 4 \ell_p/3$, at the time $t = 10 \delta t = 10 \ell_p$. The broadening of \mathcal{P}_S is clearly slower than in the standard quantum evolution,

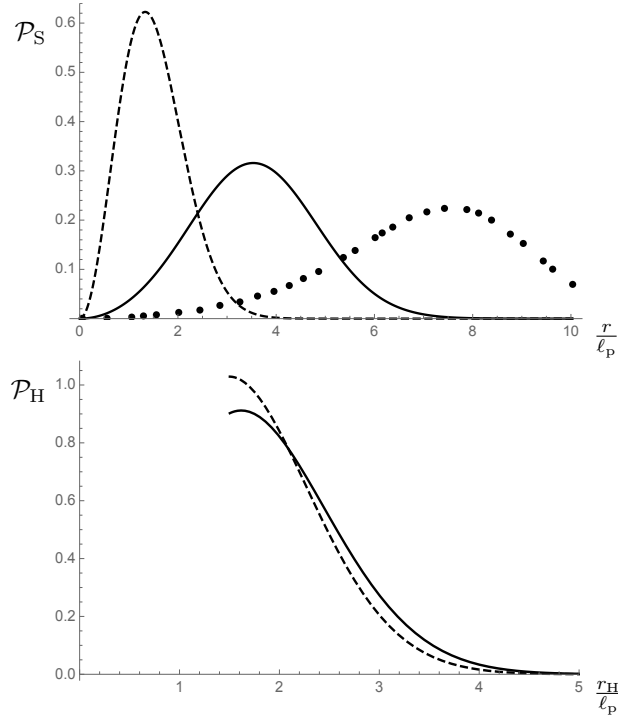
38 *R. Casadio, A. Giugno and O. Micu*


Fig. 25. Upper panel: probability density from the final wave-packet $\psi_S(r, 10 \ell_p)$ with $\ell = 4 \ell_p/3$ from the modified evolution (112) (solid line) compared to the freely evolved packet (dotted line) and initial packet $\psi_S(r, 0)$ (dashed line). Bottom panel: horizon probability density for the Gaussian particle in the upper panel at $t = 0$ (dotted line) and $t = 10 \ell_p$ (solid line). Note that $\psi_H(r_H < R_H, t) = 0$, for $R_H \equiv 1.5 \ell_p$.

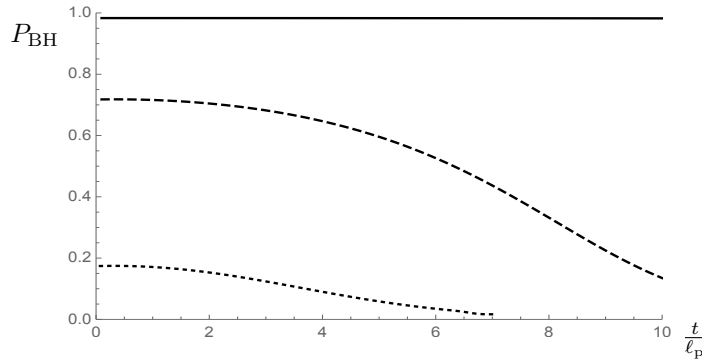


Fig. 26. Time-evolution of the probability P_{BH} for the Gaussian wave-function (21) for $\ell = \ell_p$ (solid line), $\ell = 4 \ell_p/3$ (dashed line) and $\ell = 2 \ell_p$ (dotted line).

but still leads to a decreasing BH probability density. The time evolution of the BH probability is displayed in Fig. 26 for $\lambda_m = \ell = \ell_p, 4 \ell_p/3$ and $2 \ell_p$. As usual, whenever the Gaussian width exceeds the Planck length, $\ell > \ell_p$, the BH probability

tends to vanish very fast. A possible interpretation of this result is that the initial quantum BH decays and its own Hawking radiation is simulated by the widening of the wave-function.⁴²

5. Conclusions

Since Schwarzschild solved the field equations of General Relativity and BHs entered the scene of contemporary physics, it was clear that they would have played a big role in the correspondence between large gravitational structures and the geometry of the space-time. Unfortunately, while giving very accurate corrections to Newtonian gravity, General Relativity fails at punching through the realm of quantum physics, which is renowned for giving a more reliable description of (microscopic) reality than the one given in classical terms. It seems therefore a prominent necessity to find a way which allows us to quantise the gravitational interaction (and perhaps the geometry) as our understanding of nature improves. This review introduces the reader to the investigation of the quantum properties of the geometrical structures of space-time by means of the HWF, a tool that endorses the gravitational radius with properties expected of a quantum mechanical observable.

This HQM is best elucidated by modelling a spherically symmetric massive particle with a Gaussian wave-function, which appears to be a viable description for sources around the Planck scale, that is potential quantum BHs. In fact, one finds a neutral particle is most likely inside its own horizon (i.e. the BH probability $P_{\text{BH}} \simeq 1$) when its width ℓ reaches into the quantum gravitational scale, $\ell \sim \ell_{\text{p}}$, or equivalently, the mass $m \sim m_{\text{p}}$. Moreover, the characteristic uncertainty in the horizon radius combined with the one in the size of the quantum source, results in having a GUP and a minimum measurable length (and corrections to the Hawking decay rate). This procedure is also applicable to space-times with more than one horizon, like the Reissner-Nordström metric. When the specific charge $\alpha < 1$, one finds that for a considerably broad interval of masses only the outer horizon has a large probability to form, while the probability for the inner horizon to exist is negligible. This result is counter-intuitive in the classical description and it is a phenomenological prediction resulting directly from considering the quantum nature of the causal structure of space-time. The formalism also allows one to dive into the over-charged regime, where one classically expects to have a naked singularity. It is possible to continue, albeit in a non-unique way, the HWF past the extremal $\alpha = 1$ case, but the specific charge is still limited by an upper value above which the basic properties of quantum systems, such as unitarity (which in turn follows from the normalisability of the HWF) cannot be preserved.

Forming BHs via particle collisions is a fascinating and straightforward implication of Thorne's hoop conjecture. In the strong approximation of a one-dimensional space (case in which the impact parameter is zero), the probability for a trapping surface to appear as a result of the collision between two gaussian wave-packets was computed, lending support to a quantum version of the hoop conjecture. The

main correction with respect to its classical version is that a minimum BH mass of the order of the Planck scale is again confirmed, thus pushing the BH production by particle collisions way beyond our experimental capabilities. Of course, the picture could drastically change in scenarios with extra spatial dimensions, where the fundamental gravitational mass that replaces the Planck scale could be within our reach. The HQM leads to significant corrections to the production cross-sections in the ADD models, with a possible larger and larger suppression in higher and higher dimensions. Particular emphasis was also given to lower-dimensional space-times, based on the recent claim that quantum BHs could be effectively one-dimensional objects. The HQM further supports the view that BHs in $(1+1)$ dimension cannot indeed be classical.

Most of the review has dealt with static configurations, and even the case of particle collisions was treated in this perspective. However, one should not forget the proper (classical) meaning of a horizon is to trap matter inside of it, and one can hardly overlook how this property must affect the time-evolution of the system deeply. A possible time-dependent HQM is governed by a modified Schrödinger equation, in which the probability for the particle to lie inside its own horizon affects the evolution in such a way that a state with probability $P_{\text{BH}} = 1$ does no longer evolve in time. As expected, even on qualitative grounds, this modified quantum dynamics slows down the spread of a Gaussian packet.

The above cases show some of the uses of the HQM and open up many perspectives for future works. First of all, one could apply the HQM to simple models of spherically symmetric gravitational collapse and estimate the chance that it actually leads to the formation of a BH. After extending the formalism to electrically charged wave-packets, the next natural thing to do is then to investigate rotating sources. This extensions is important for quantum BHS because elementary particles can have non-vanishing spin, and because the impact parameter in particle collisions is generally not zero, so that the resulting BH is expected to have angular momentum in most physical cases.

Acknowledgments

It is a pleasure to thank X. Calmet, R.T. Cavalcanti, J. Mureika, A. Orlandi, F. Scardigli, D. Stojkovic for fruitful collaboration, and A. Davidson, G. Dvali, A. Giusti, C. Gomez, B. Harms, F. Kuhnel, P. Nicolini, N. Wintergerst for stimulating discussions. R. C. and A. G. are partly supported by the INFN grant FLAG.

Appendix A. Useful integrals

In this review, we made use of integrals of the form

$$I_3 = \int_1^\infty \gamma \left(\frac{3}{2}, Ax^2 \right) e^{-x^2} x^2 dx \quad (\text{A.1})$$

where A is a positive real parameter. From

$$x e^{-x^2} = -\frac{1}{2} \frac{d}{dx} e^{-x^2} \quad (\text{A.2})$$

and

$$\frac{d}{dy} \gamma(s, y) = y^{s-1} e^{-y}, \quad (\text{A.3})$$

upon integrating by parts, one obtains

$$\begin{aligned} I_3 &= \int_1^\infty \gamma\left(\frac{3}{2}, A^2 x^2\right) e^{-x^2} x^2 dx \\ &= \frac{1}{2e} \gamma\left(\frac{3}{2}, A^2\right) + \frac{1}{2} \int_1^\infty e^{-x^2} \frac{d}{dx} \left[x \gamma\left(\frac{3}{2}, A^2 x^2\right) \right] dx \\ &= \frac{1}{2e} \gamma\left(\frac{3}{2}, A^2\right) + A^3 \int_1^\infty e^{-(1+A^2)x^2} x^3 dx + \frac{1}{2} \int_1^\infty e^{-x^2} \gamma\left(\frac{3}{2}, A^2 x^2\right) dx \\ &= \frac{1}{2e} \gamma\left(\frac{3}{2}, A^2\right) + \frac{A^3 \Gamma(2, 1+A^2)}{2(1+A^2)^2} + \frac{1}{2} \int_1^\infty e^{-x^2} \gamma\left(\frac{3}{2}, A^2 x^2\right) dx, \end{aligned} \quad (\text{A.4})$$

From the property

$$\begin{aligned} \gamma\left(\frac{3}{2}, A^2 x^2\right) &= \frac{1}{2} \gamma\left(\frac{1}{2}, A^2 x^2\right) - A x e^{-A^2 x^2} \\ &= \frac{\sqrt{\pi}}{2} \operatorname{erf}(Ax) - A x e^{-A^2 x^2}, \end{aligned} \quad (\text{A.5})$$

the integral

$$\begin{aligned} \int_1^\infty e^{-x^2} \gamma\left(\frac{3}{2}, A^2 x^2\right) dx &= \frac{\sqrt{\pi}}{2} \int_1^\infty \operatorname{erf}(Ax) e^{-x^2} dx - A \int_1^\infty e^{-(1+A^2)x^2} dx \\ &= -\frac{A e^{-(1+A^2)}}{2(1+A^2)} + \frac{\pi}{4} [1 - \operatorname{erf}(1) \operatorname{erf}(A)] \\ &\quad - \pi T\left(\sqrt{2} A, \frac{1}{A}\right), \end{aligned} \quad (\text{A.6})$$

where $\operatorname{erf}(x)$ is an error function and $T(a, b)$ is the Owen's T distribution defined as

$$T(a, b) = \frac{1}{2\pi} \int_0^a \frac{e^{-\frac{1}{2} b^2 (1+x^2)}}{1+x^2} dx. \quad (\text{A.7})$$

42 *R. Casadio, A. Giugno and O. Micu*

Finally, putting everything together yields

$$\begin{aligned}
I_3 &= \frac{1}{2e} \gamma \left(\frac{3}{2}, A^2 \right) + \frac{\pi}{8} [1 - \operatorname{erf}(1) \operatorname{erf}(A)] + \frac{A^3 \Gamma(2, 1 + A^2)}{2(1 + A^2)^2} \\
&\quad - \frac{A e^{-(1+A^2)}}{4(1 + A^2)} - \frac{\pi}{2} T \left(\sqrt{2} A, \frac{1}{A} \right) \\
&= \frac{\pi}{8} \operatorname{erfc}(A) + \frac{\sqrt{\pi}}{4} \Gamma \left(\frac{3}{2}, 1 \right) \operatorname{erf}(A) - \frac{A}{2} e^{-(1+A^2)} + \frac{A^3 (2 + A^2) e^{-(1+A^2)}}{2(1 + A^2)^2} \\
&\quad - \frac{A e^{-(1+A^2)}}{4(1 + A^2)} - \frac{\pi}{2} T \left(\sqrt{2} A, \frac{1}{A} \right) \\
&= \frac{\pi}{8} \operatorname{erfc}(A) + \frac{\sqrt{\pi}}{4} \Gamma \left(\frac{3}{2}, 1 \right) \operatorname{erf}(A) - \frac{A(3 + A^2)}{4(1 + A^2)^2} e^{-(1+A^2)} \\
&\quad - \frac{\pi}{2} T \left(\sqrt{2} A, \frac{1}{A} \right). \tag{A.8}
\end{aligned}$$

References

1. A. Einstein, *Annalen Phys.* **17** (1905) 891 [*Annalen Phys.* **14** (2005) 194].
2. A. Einstein, *Annalen Phys.* **49** (1916) 769 [*Annalen Phys.* **14** (2005) 517].
3. A. D. Sakharov, *Sov. Phys. Dokl.* **12** (1968) 1040 [*Dokl. Akad. Nauk Ser. Fiz.* **177** (1967) 70] [*Sov. Phys. Usp.* **34** (1991) 394] [*Gen. Rel. Grav.* **32** (2000) 365].
4. P. A. M. Dirac, *Proc. Roy. Soc. Lond. A* **246** (1958) 333.
5. P. Bergmann, *Phys. Rev.* **144** (1966) 1078.
6. B.S. DeWitt, *Phys. Rev.* **160** (1967) 1113-1148.
7. C. Rovelli, *Living Rev. Rel.* **1** (1998) 1.
8. G. Lemaître, *Ann. Soc. Sci. Bruxelles A* **53** (1933) 51.
9. P.C. Vaidya, *Proc. Indian Acad. Sci., Sect. A, Phys. Sci.* **33** (1951a) 254.
10. C.W. Misner, *Phys. Rev. B* **137** (1965) 1350;
11. R.W. Linquist, C.W. Misner and R.A. Schwartz, *Phys. Rev. B* **137** (1965) 1364.
12. J.R. Oppenheimer and H. Snyder, *Phys. Rev.* **56** (1939) 455.
13. J.R. Oppenheimer and G.M. Volkoff, *Phys. Rev.* **55** (1939) 374.
14. R. Penrose, *Riv. Nuovo Cim.* **1** (1969) 252 [*Gen. Rel. Grav.* **34** (2002) 1141].
15. E. Poisson and W. Israel, *Phys. Rev. D* **41** (1990) 1796.
16. P.S. Joshi, “Gravitational Collapse and Spacetime Singularities,” *Cambridge Monographs on Mathematical Physics* (Cambridge, 2007).
17. J.D. Bekenstein, “Black holes: Physics and astrophysics. Stellar-mass, supermassive and primordial black holes,” *astro-ph/0407560*.
18. N. D. Birrell and P. C. W. Davies, “Quantum Fields in Curved Space,” *Cambridge Monographs on Mathematical Physics* (Cambridge, 1984).
19. S.W. Hawking, *Nature* **248**, 30 (1974).
20. S.W. Hawking, *Comm. Math. Phys.* **43**, 199 (1975).
21. K.S. Thorne, “Nonspherical Gravitational Collapse: A Short Review,” in *J.R. Klauder, Magic Without Magic*, San Francisco (1972), 231.
22. P. D. D’Eath and P. N. Payne, *Phys. Rev. D* **46** (1992) 658.
23. P. D. D’Eath and P. N. Payne, *Phys. Rev. D* **46** (1992) 675.
24. P. D. D’Eath and P. N. Payne, *Phys. Rev. D* **46** (1992) 694.
25. J.M.M. Senovilla, *Europhys. Lett.* **81** (2008) 20004.

26. G.L. Alberghi, R. Casadio, O. Micu and A. Orlandi, *JHEP* **1109** (2011) 023.
27. S.D.H. Hsu, *Phys. Lett. B* **555** (2003) 92.
28. B. J. Carr and S. B. Giddings, *Sci. Am.* **292N5** (2005) 30 [*Spektrum Wiss.* **2005N9** (2005) 32].
29. X. Calmet, D. Fragkakis and N. Gausmann, *Eur. Phys. J. C* **71** (2011) 1781;
30. X. Calmet, W. Gong and S.D.H. Hsu, *Phys. Lett. B* **668** (2008) 20.
31. X. Calmet, *Mod. Phys. Lett. A* **29** (2014) 1450204.
32. X. Calmet and R. Casadio, *Eur. Phys. J. C* **75** (2015) 9, 445
33. R. Casadio, "Localised particles and fuzzy horizons: A tool for probing Quantum Black Holes," arXiv:1305.3195 [gr-qc].
34. M. Maggiore, *Phys. Lett. B* **319** (1993) 83.
35. A. Kempf, G. Mangano, R.B. Mann, *Phys. Rev. D* **52** (1995) 1108.
36. R. Casadio and F. Scardigli, *Eur. Phys. J. C* **74** (2014) 1, 2685.
37. F. Scardigli, *Phys. Lett. B* **452** (1999) 39.
38. R. Casadio and F. Scardigli, *Class. Quant. Grav.* **20** (2003) 3915.
39. R. Casadio and F. Scardigli, *Int. J. Mod. Phys. D* **18** (2009) 319.
40. M. Bleicher, P. Nicolini, M. Sprenger, *Eur. J. Phys.* **33** (2012) 853.
41. R. Casadio, A. Giugno, O. Micu and A. Orlandi, *Entropy* **17** (2015) 6893.
42. R. Casadio, *Eur. Phys. J. C* **75** (2015) 160.
43. R. Casadio, R.T. Cavalcanti, A. Giugno and J. Mureika, "Horizon of quantum black holes in various dimensions," arXiv:1509.09317 [gr-qc].
44. R. Casadio, O. Micu and D. Stojkovic, *JHEP* **1505** (2015) 096.
45. R. Casadio, O. Micu and D. Stojkovic, *Phys. Lett. B* **747** (2015) 68.
46. R. Casadio, O. Micu and F. Scardigli, *Phys. Lett. B* **732** (2014) 105.
47. K. Schwarzschild, *Sitzungsber. Preuss. Akad. Wiss. Berlin (Math. Phys.)* **1916** (1916) 189.
48. K. Schwarzschild, *Sitzungsber. Preuss. Akad. Wiss. Berlin (Math. Phys.)* **1916** (1916) 424.
49. H. Stephani, "Relativity: An introduction to special and general relativity," Cambridge University Press (Cambridge, 2004).
50. V. Faraoni, "Is the Hawking quasilocal energy Newtonian?," arXiv:1510.03789 [gr-qc].
51. G. Dvali, C. Gomez and A. Kehagias, *JHEP* **1111** (2011) 070.
52. G. Dvali, G.F. Giudice, C. Gomez and A. Kehagias, *JHEP* **1108** (2011) 108.
53. S. Hossenfelder, *Living Rev. Rel.* **16** (2013) 2.
54. B. S. DeWitt, *Phys. Rev.* **162** (1967) 1195. doi:10.1103/PhysRev.162.1195
55. K. Nakamura, S. Konno, Y. Oshiro and A. Tomimatsu, *Prog. Theor. Phys.* **90** (1993) 861.
56. A. Ashtekar, J. Baez, A. Corichi and K. Krasnov, *Phys. Rev. Lett.* **80** (1998) 904.
57. S. Carlip, *Phys. Rev. Lett.* **82** (1999) 2828.
58. R. H. Price and K. S. Thorne, *Phys. Rev. D* **33**, 915 (1986).
59. K. S. Thorne, R. H. Price and D. A. Macdonald, "Black Holes: The Membrane Paradigm," Yale University Press (New Haven, 1986).
60. C. R. Stephens, G. 't Hooft and B. F. Whiting, *Class. Quant. Grav.* **11** (1994) 621.
61. L. Susskind, *J. Math. Phys.* **36** (1995) 6377.
62. P. Hajicek, *Phys. Rev. D* **30** (1984) 1178.
63. A. Tomimatsu, *Phys. Lett. B* **289** (1992) 283.
64. R. Casadio, *Phys. Lett. B* **511** (2001) 285.
65. K. V. Kuchar, *Phys. Rev. D* **50** (1994) 3961.
66. A. Davidson and B. Yellin, *Phys. Lett. B* **736** 267.

67. R. Brustein and A. J. M. Medved, *JHEP* **1406** (2014) 057.
68. G. Dvali and C. Gomez, *Fortsch. Phys.* **61** (2013) 742.
69. G. Dvali and C. Gomez, *JCAP* **01** (2014) 023 .
70. G. Dvali and C. Gomez, *Eur. Phys. J. C* **74** (2014) 2752.
71. G. Dvali and C. Gomez, *Phys. Lett. B* **716**, (2102) 240.
72. F. Kühnel and B. Sundborg, *JHEP* **1412** (2014) 016.
73. R. Casadio and A. Orlandi, *JHEP* **1308** (2013) 025.
74. R. Casadio, A. Giugno, O. Micu and A. Orlandi, *Phys. Rev. D* **90** (2014) 8, 084040.
75. W. Mück and G. Pozzo, *JHEP* **1405** (2104) 128.
76. R. Casadio, A. Giugno and A. Orlandi, *Phys. Rev. D* **91** (2015) 12, 124069.
77. R. Di Criscienzo, S.A. Hayward, M. Nadalini, L. Vanzo and S. Zerbini, *Class. Quant. Grav.* **26** (2009) 062001.
78. F. Scardigli, *Nuovo Cim. B* **110** (1995) 1029.
79. R.J. Adler, P. Chen and D.I. Santiago, *Gen. Rel. Grav.* **33** (2001) 2101.
80. M. Cavaglia, S. Das and R. Maartens, *Class. Quant. Grav.* **20** (2003) L205.
81. F. Scardigli, “Hawking temperature for various kinds of black holes from Heisenberg uncertainty principle”, gr-qc/0607010.
82. K. Nouicer, *Class. Quant. Grav.* **24**, (2007) 5917.
83. F. Scardigli, “Glimpses on the micro black hole planck phase”, arXiv:0809.1832 [hep-th].
84. P. Chen, C. Gruber and F. Scardigli, *Phys. Rev. D* **83**, (2011) 063507.
85. P. Jizba, H. Kleinert, F. Scardigli, *Phys. Rev. D* **81**, (2010) 084030.
86. M.K. Parikh and F. Wilczek, *Phys. Rev. Lett.* **85**, (2000) 5042.
87. M. Angheben, M. Nadalini, L. Vanzo and S. Zerbini, *JHEP* **0505**, (2005) 014.
88. R. Casadio and B. Harms, *Phys. Rev. D* **58** (1998) 044014.
89. R. Casadio and B. Harms, *Entropy* **13** (2011) 502.
90. E. Greenwood and D. Stojkovic, *JHEP* 032P 0408.
91. A. Saini and D. Stojkovic, *Phys. Rev. D* **89** (2014) 044003.
92. L. M. Krauss, D. Stojkovic and T. Vachaspati, *Phys. Rev. D* **76** (2007) 024005.
93. D. Stojkovic and T. Vachaspati, *Phys. Lett. B* **663** (2008) 107.
94. E. Greenwood, D. Stojkovic and J. E. Wang, *Phys. Rev. D* **80** (2009) 124027.
95. H. Reissner, *Annalen der Phys.* **50** (1916) 106.
96. G. Nordström, *Verhandl. Koninkl. Ned. Akad. Wetenschap., Afdel. Natuurk.*, **26** (1918) 1201.
97. V. I. Dokuchaev, *Class. Quant. Grav.* **31** (2014) 055009.
98. E. Brown and R. B. Mann, *Phys. Lett. B* **694** (2011) 440.
99. E. G. Brown, R. B. Mann and L. Modesto, *Phys. Rev. D* **84** (2011) 104041.
100. S. B. Giddings and S. D. Thomas, *Phys. Rev. D* **65** (2002) 056010.
101. S. Dimopoulos and G. L. Landsberg, *Phys. Rev. Lett.* **87** (2001) 161602.
102. N. Arkani-Hamed, S. Dimopoulos and G. R. Dvali, *Phys. Lett. B* **429** (1998) 263.
103. I. Antoniadis, N. Arkani-Hamed, S. Dimopoulos and G. R. Dvali, *Phys. Lett. B* **436** (1998) 257.
104. L. Randall and R. Sundrum, *Phys. Rev. Lett.* **83** (1999) 3370.
105. L. Randall and R. Sundrum, *Phys. Rev. Lett.* **83** (1999) 4690.
106. K. Koyama and R. Maartens, *Living Rev. Rel.* **13** (2010) 5.
107. J. R. Mureika, *Phys. Lett. B* **716**, 171 (2012).
108. R. Loll, *Nucl. Phys. Proc. Suppl.* **94** (2001) 96.
109. J. Ambjorn, J. Jurkiewicz, R. Loll, *Phys. Rev. D* **72** (2005) 064014.
110. J. Ambjorn, J. Jurkiewicz, R. Loll, “Quantum Gravity, or The Art of Building Space-time,” in *Approaches to Quantum Gravity*, ed. D. Oriti, Cambridge University Press

- (2006).
111. L. Modesto and P. Nicolini, *Phys. Rev. D* **81** (2010) 104040.
 112. P. Nicolini and E. Spallucci, *Adv. High Energy Phys.* **2014** (2014) 805684.
 113. B. J. Carr, J. Mureika and P. Nicolini, *JHEP* **1507** (2015) 052.
 114. J. Mureika and P. Nicolini, *Eur. Phys. J. Plus* **128** (2013) 78.
 115. L.A. Anchordoqui, D.C. Dai, M. Fairbairn, G. Landsberg and D. Stojkovic, *Mod. Phys. Lett. A* **27** (2102) 1250021.
 116. L.A. Anchordoqui, D.C. Dai, H. Goldberg, G. Landsberg, G. Shaughnessy, D. Stojkovic and T.J. Weiler, *Phys. Rev. D* **83** (2011) 114046.
 117. J.R. Mureika and D. Stojkovic, *Phys. Rev. Lett.* **106** (2011) 101101.
 118. J.R. Mureika and D. Stojkovic, *Phys. Rev. Lett.* **107** (2011) 169002.
 119. N. Afshordi and D. Stojkovic, *Phys. Lett. B* **739** (2014) 117.
 120. D. Stojkovic, *Mod. Phys. Lett. A* **28** (2013) 1330034.